

Cite this: *Chem. Sci.*, 2022, 13, 13368

All publication charges for this article have been paid for by the Royal Society of Chemistry

Syntheses, homeomorphic and configurational isomerizations, and structures of macrocyclic aliphatic dibridgehead diphosphines; molecules that turn themselves inside out†

Yun Zhu, , Michael Stollenz, ‡ Samuel R. Zarcone, Sugam Kharel, Hemant Joshi, § Nattamai Bhuvanesh, Joseph H. Reibenspies and John A. Gladysz *

The diphosphine complexes *cis*- or *trans*- $\text{PtCl}_2(\text{P}((\text{CH}_2)_n)_3\text{P})$ ($n = \text{b}/12, \text{c}/14, \text{d}/16, \text{e}/18$) are demetallated by $\text{MC}\equiv\text{X}$ nucleophiles to give the title compounds $\text{P}((\text{CH}_2)_n)_3\text{P}$ (**3b–e**, 91–71%). These “empty cages” react with PdCl_2 or PtCl_2 sources to afford *trans*- $\text{MCl}_2(\text{P}((\text{CH}_2)_n)_3\text{P})$. Low temperature ^{31}P NMR spectra of **3b** and **c** show two rapidly equilibrating species (**3b**, 86 : 14; **3c**, 97 : 3), assigned based upon computational data to *in,in* (major) and *out,out* isomers. These interconvert by homeomorphic isomerizations, akin to turning articles of clothing inside out (**3b/c**: ΔH^\ddagger 7.3/8.2 kcal mol $^{-1}$, ΔS^\ddagger –19.4/–11.8 eu, minor to major). At 150 °C, **3b**, **c**, **e** epimerize to (60–51) : (40–49) mixtures of (*in,in/out,out*) : *in,out* isomers, which are separated via the bis(borane) adducts **3b**, **c**, **e**·2BH $_3$. The configurational stabilities of *in,out*-**3b**, **c**, **e** preclude phosphorus inversion in the interconversion of *in,in* and *out,out* isomers. Low temperature ^{31}P NMR spectra of *in,out*-**3b**, **c** reveal degenerate *in,out/out,in* homeomorphic isomerizations ($\Delta G^\ddagger_{\text{c}}$ 12.1, 8.5 kcal mol $^{-1}$). When (*in,in/out,out*)-**3b**, **c**, **e** are crystallized, *out,out* isomers are obtained, despite the preference for *in,in* isomers in solution. The lattice structures are analyzed, and the D_3 symmetry of *out,out*-**3c** enables a particularly favorable packing motif. Similarly, (*in,in/out,out*)-**3c**, **e**·2BH $_3$ crystallize in *out,out* conformations, the former with a cycloalkane solvent guest inside.

Received 24th August 2022
Accepted 13th October 2022

DOI: 10.1039/d2sc04724a

rsc.li/chemical-science

Introduction

Bicyclic compounds with two bridgehead heteroatoms are quite common for nitrogen but less familiar for other elements. The many dinitrogen examples include DABCO (1,4-diazobicyclo [2.2.2]octane), cryptands,¹ and the macrocyclic diprotonated diamines **I** (Scheme 1).² The last group represents touchstones for many of the phenomena detailed below.² In contrast, the

corresponding aliphatic dibridgehead diphosphines, or Brønsted or Lewis acid adducts thereof, are much less explored. Prior to the work herein, compounds of the formula $\text{P}((\text{CH}_2)_n)_3\text{P}$ were unknown for $n > 4$.³

Macrocyclic versions of such molecules, as well as analogs with carbon bridgeheads, can exist as *in/out* isomers⁴ differing in the relative orientations of the bridgehead substituents. As shown for **I** (Scheme 1), four limits apply: *in,in*, *out,out*, *in,out*, and *out,in*. When the northern and southern hemispheres are identical, the last two are degenerate. For structures that lack a C_3 axis, *in/out* geometries can be assigned from the angles defined by the two bridgehead atoms and their substituents, as shown in **II**. For some time, *in/out* isomerism has been a curiosity, but the phenomenon has now been coupled to function, for example in the selective transport of metal dichloride fragments.⁵

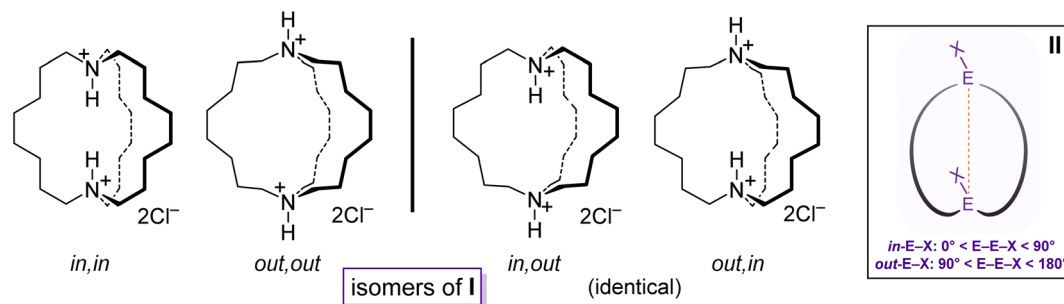
The diprotonated dibridgehead diamines **I** represent the historical “ground zero” for the study of homeomorphic isomerization.⁴ This terminology, imported from the field of topology,⁶ denotes a dynamic process that is tantamount to turning a molecule inside out. Essentially, one of the tethers connecting the bridgehead atoms is “pulled through” the macrocycle defined by the other two, like reaching inside

Department of Chemistry, Texas A&M University, PO Box 30012, College Station, Texas, 77842-3012, USA. E-mail: gladysz@mail.chem.tamu.edu

† Electronic supplementary information (ESI) available: Additional preparative, crystallographic, NMR, and rate data, and a video representing the interconversion of **III**, **IV**, and **VI** in Scheme 2. The EX (or P) bridgeheads are depicted as triangles, initially with the blue sides “in” and the white sides “out”. Threading one $(\text{CH}_2)_n$ chain through the macrocycle defined by the other two reverses these relationships (without pyramidal inversion or bond-breaking). This is termed “homeomorphic isomerization”. CCDC 2190116 (*out,out*-**3b**), 2190438 (*out,out*-**3c**), 2190439 (*out,out*-**3e**), and 2190440 (*out,out*-**3e**·2BH $_3$). For ESI and crystallographic data in CIF or other electronic format see DOI: <https://doi.org/10.1039/d2sc04724a>

‡ Current address: Department of Chemistry and Biochemistry, Kennesaw State University 370 Paulding Avenue NW, MD #1203, Kennesaw, GA 30144, USA.

§ Current address: Department of Chemistry, School of Chemical Sciences and Pharmacy, Central University of Rajasthan, Ajmer, Rajasthan 305817 India.



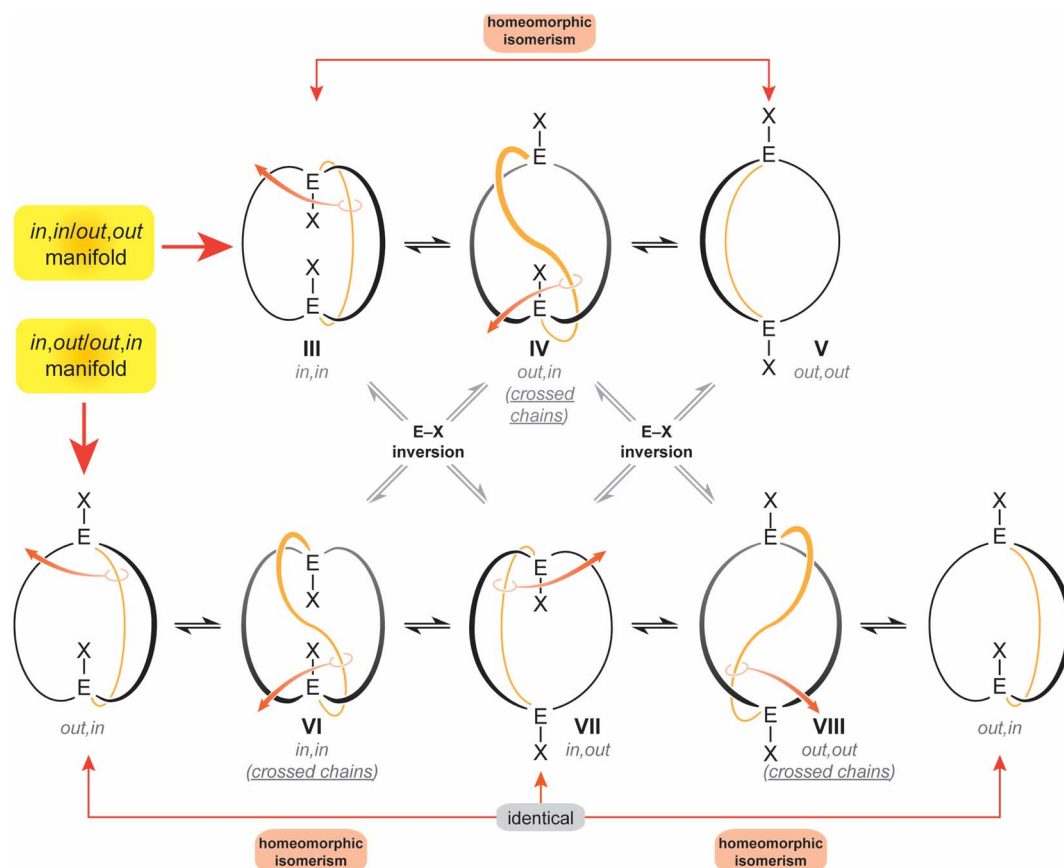
Scheme 1 Dibridgehead diammonium salts that illustrate the limiting types of *in/out* isomers (I), and geometric criteria for *in/out* bridgeheads EX (II).

a rubber glove and pulling the inner surface outside. As depicted in Scheme 2 as well as a video (ESI[†]), this interconverts *in,in* and *out,out* isomers, and *in,out* and *out,in* isomers – in both cases, an apparent inversion of configuration at each bridgehead atom.⁷

Interestingly, data for the *in,in*, *out,out* and *in,out* equilibria of the diprotonated dibridgehead diamines **I** (Scheme 1) implicated an alternative mechanism: namely, proton dissociation, pyramidal inversion of the resulting trivalent nitrogen atom, and nitrogen reprotonation.² Indeed, when the bridgeheads are trivalent group 15 heteroatoms (E:), simple pyramidal

inversion can effect *in/out* isomerization, as represented by the “×” pathways connecting the upper and lower manifolds in Scheme 2. However, in the absence of unprecedented cooperative phenomena, only *one inversion at a time* would be expected, and given well established trends in inversion barriers,^{8,9} this would be rapid at room temperature only in the case of nitrogen.

For the sake of completeness, three species with “crossed chains” (**IV**, **VI**, **VIII**) are also depicted in Scheme 2. The conformational details of these isomerizations remain beyond the scope of this study, but such architectures receive support in



Scheme 2 Conventional *in,in* (III), *out,out* (V), and *in,out* (VIII) isomers of a bicyclo[z.z.z] system with EX bridgeheads, and “crossed chain” variants IV, VII and VIII.



dynamic simulation computations, which locate abundant numbers of local minima.¹⁰ As exemplified in the Discussion section, isomers of the type **VIII** have been isolated for P–X and Si–X systems with sterically demanding X groups.^{11–13} In all of these contexts, the “inside out” nature of homeomorphic isomerization means that functionality might be directed in a convergent manner towards an interior domain in one conformation, and externally in the other.

Apart from this work, only five molecular systems have been definitively shown to undergo homeomorphic isomerization,^{4,14,15} as defined by (1) the ability to observe both *in,in* and *out,out* forms and establish a direct path between them, or (2) the ability to observe inequivalent bridgehead atoms of an *in,out* isomer (the E–X in **VII** are not related by a symmetry operation), and their exchange at higher temperatures. In other cases, there can be a strong inference of homeomorphic isomerization from NMR properties, but with data for both limits remaining elusive.^{12,16,17} Particularly noteworthy are earlier efforts by Habicher and Bauer that encompass several types of bicyclic dibridgehead diphosphorus compounds with *p*-phenylene linkers in the tethers.^{16,17} They and Alder⁴ were pioneers in articulating some of the concepts expressed above.

Previous synthetic studies from the authors' laboratory lay the groundwork for the effort detailed herein. As shown in Scheme 3 (top), platinum dichloride complexes with two *trans* or *cis* alkene containing phosphines of the formula $P((CH_2)_mCH=CH_2)_3$ undergo three fold intramolecular ring closing metathesis when treated with Grubbs' catalyst.^{18,19} Subsequent hydrogenations give what are termed “gyroscope-like” (*trans*) or “parachute-like” (*cis*) complexes in modest yields. The *trans* isomers are adducts of *in,in* dibridgehead diphosphine ligands, and the *cis* isomers adducts of *out,out* ligands. This underscores the appreciable conformational flexibility of the ligands.

In this paper, we report (1) the facile liberation of four aliphatic dibridgehead diphosphine ligands $P((CH_2)_n)_3P$ (**3**) from **2**, (2) detailed variable temperature NMR analyses of **3**, which in some cases allow the observation of distinct *in,in* and *out,out* isomers, (3) thermal epimerisations that equilibrate the *in,in/out,out* mixtures and *in,out* isomers, (4) the formation and deprotection of the corresponding bis(borane) adducts, (5) six crystals structures, and in-depth analyses thereof. Companion computational investigations that support certain assignments also deserve emphasis.^{10,20} Small portions of these data have been communicated, CCDC 838916 (*out,out*-**3c**· BH_3 ·($C_5H_9CH_3$)) and CCDC 838917 (*out,out*-**3c**· $2BH_3$ ·($C_6H_{11}CH_3$)).^{5,21}

Results

Syntheses of title compounds **3**

As shown in Scheme 3 (bottom), the platinum dichloride complex *trans*-**2c** was treated with excesses of $NaC\equiv CH$, $LiC\equiv CPh$, or $KC\equiv N$. Workups gave the dibridgehead diphosphine **3c** ($n = 14$) in 86–91% yields. In the reaction with $KC\equiv N$, the concurrent formation of $K_2Pt(C\equiv N)_4$ was verified by $^{13}C\{^1H\}$ NMR and X-ray crystallography. In that with $LiC\equiv CPh$, the salt $Li_2Pt(C\equiv CPh)_4 \cdot 4THF$ could be isolated in 35% yield. A sample

was independently synthesized from the reaction of $LiC\equiv CPh$ and $PtCl_2(THT)_2$ (THT = tetrahydrothiophene). Similar reactions of *cis*-**2b**, **d** and *trans*-**2e** with $KC\equiv N$ gave the diphosphines **3b**, **d**, **e** in 71–85% yields. These feature 26- to 38-membered macrocycles.

Compounds **3b–e** were isolated as low melting white solids that were moderately air sensitive, especially in solution.²² They were characterized by NMR spectroscopy (1H , $^{13}C\{^1H\}$, $^{31}P\{^1H\}$) and other techniques as described below. Data are summarized in the Experimental section. The three $PCH_2CH_2CH_2$ $^{13}C\{^1H\}$ NMR signals showed comparable $^nJ_{CP}$ values (10–12 Hz), but more detailed assignments could not be made with certainty. Several *cis*- $PtCl_2$ (diphosphine) species similarly react with excess $KC\equiv N$ to give $K_2Pt(C\equiv N)_4$.²³

Probes of stereochemistry and dynamic behavior

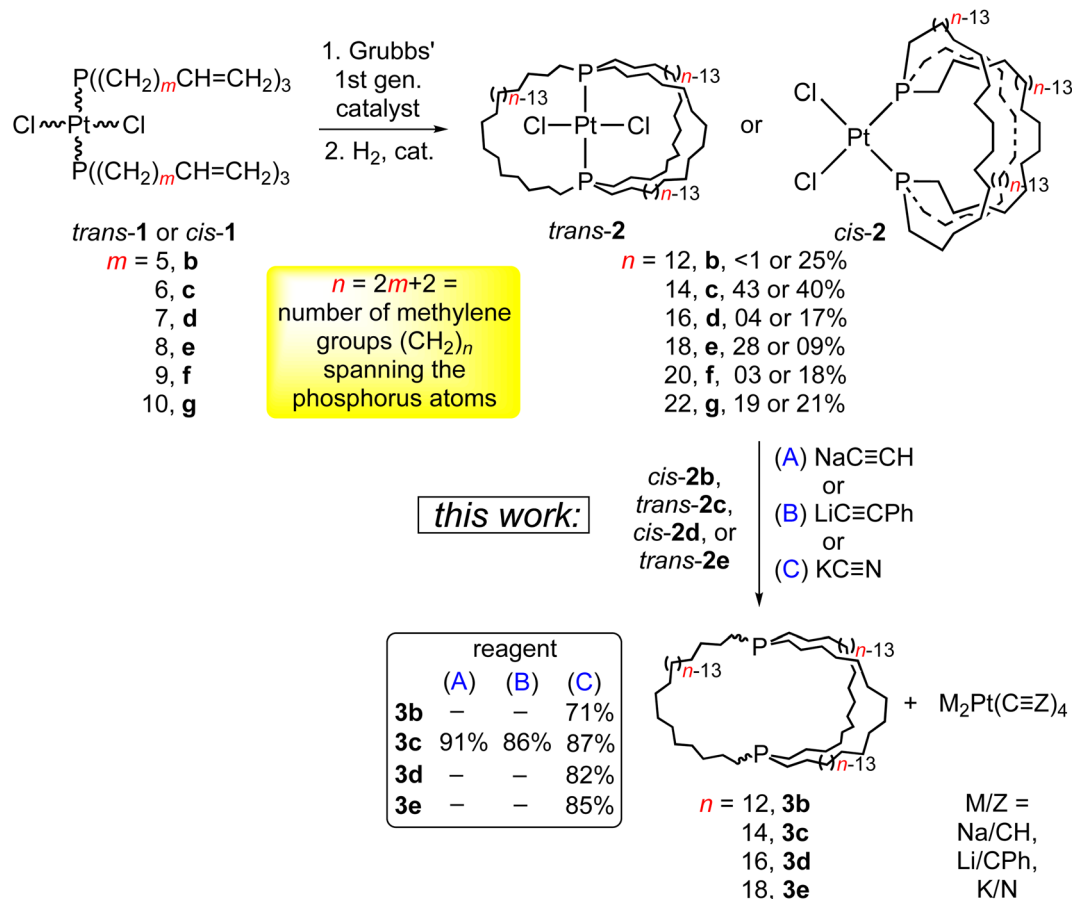
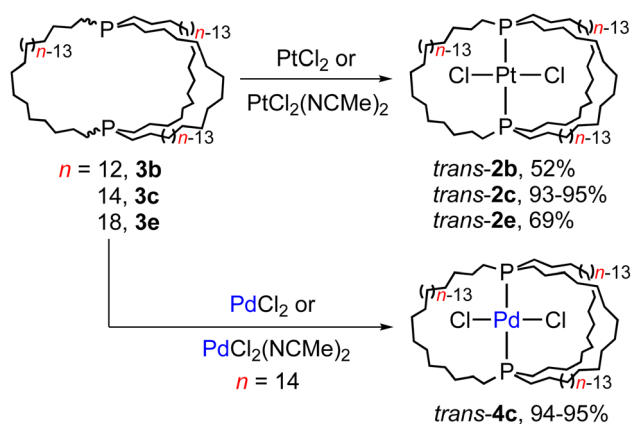
One initial question concerns the distribution of *in/out* stereoisomers of **3b–e** produced in Scheme 3. The diphosphine ligands in *trans*-**2c**, **e** and *cis*-**2b**, **d** have *in,in* and *out,out* orientations, respectively, and the corresponding free ligands can interconvert by homeomorphic isomerizations as summarized in Scheme 2. As shown in Scheme 4, the diphosphines **3b**, **c**, **e** reacted with $PtCl_2$ sources to generate the gyroscope-like platinum complexes *trans*-**2b**, **c**, **e**. Comparable reactions of **3c** and $PdCl_2$ sources afforded *trans*-**4c**, which had been previously synthesized by a route analogous to *trans*-**2c**.^{18a} Importantly, *trans*-**2b** is a new compound, unavailable in significant quantities by the direct route in Scheme 3.

Trialkylphosphines normally exhibit appreciable pyramidal inversion barriers ($\Delta G_{403\text{ K}}^\ddagger = 32\text{--}35\text{ kcal mol}^{-1}$),⁸ with temperatures of $\geq 140^\circ\text{C}$ typically required to effect racemization or epimerization. Hence, the efficient reconstitution of *trans*-**2c**, **e** under mild conditions in Scheme 4 seemingly excludes the formation of *in,out*-**3b–e** in Scheme 3. In separate studies, *trans*-**2c–e** have been shown to be much more stable than *cis*-**2c–e** (equilibration at *ca.* 160°C , with ΔG for **2c** 3–12 kcal mol^{-1} depending upon the medium and temperature by DFT).^{19,24} Hence, the absence of *cis* products in Scheme 4 is not surprising.

In the course of characterizing the reactivity of **3b–e**, low temperature $^{31}P\{^1H\}$ NMR spectra were acquired. When toluene or toluene- d_8 solutions of **3c** were cooled, a small upfield peak reproducibly appeared as depicted in Fig. 1a and S1 (ESI†). The line widths for the major signal varied strongly ($w_{1/2}$ 5.8 to 93.0 Hz, 300 K to 233 K, decreasing to 6.3 Hz at 193 K; Fig. S5, ESI†). A ^{31}P EXSY experiment (Fig. S2†) confirmed that the species responsible for the two peaks are in equilibrium. The area ratio at 193 K (-80°C), 97 : 3, corresponded to a $\Delta G_{193\text{ K}}$ value of 1.33 kcal mol^{-1} .

The smaller macrocycle **3b** also exhibited two signals in toluene- d_8 at lower temperatures (Fig. 1b and S3†). At 213 K (-60°C), integration indicated a 86 : 14 isomer ratio, for a $\Delta G_{213\text{ K}}$ value of 0.77 kcal mol^{-1} , with the downfield signal again dominant. These coalesced at approximately 303 K (30°C), and $^{13}C\{^1H\}$ NMR signals also sharpened above this temperature (Fig. S4†). Two $^{31}P\{^1H\}$ NMR signals were also



Scheme 3 Syntheses of the title compounds (**3b–e**) from platinum complexes.Scheme 4 Reactions of title compounds with MCl₂ sources.

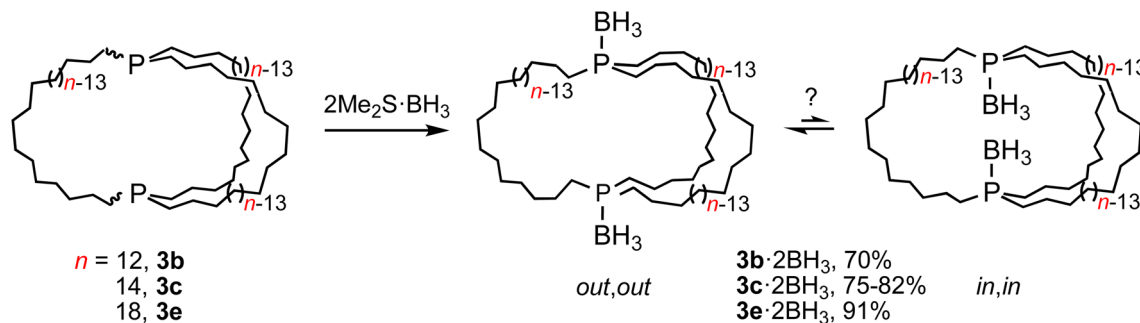
observed in mesitylene (85 : 15, 213 K; T_c near 313 K) and THF (91 : 9, 213 K; T_c near 263 K).²⁵ For both **3b** and **c**, the spectra were simulated, as exemplified for **3b** in Fig. 1b and S3.† Eyring plots of the rate constants derived from the line shapes²⁶ (Fig. S7†) gave ΔH^\ddagger and ΔS^\ddagger values of 7.3 kcal mol^{−1} and −19.4 eu for **3b** (minor to major; $\Delta G_{213\text{ K}}^\ddagger = 11.4$ kcal mol^{−1} or 12.1 kcal mol^{−1} major to minor), and 8.2 kcal mol^{−1} and −11.8 eu for **3c** (minor to major; $\Delta G_{193\text{ K}}^\ddagger = 10.4$ kcal mol^{−1}, or 11.5 major to minor).²⁶

Accordingly, the two ³¹P{¹H} NMR signals are attributed to *in,in* and *out,out* isomers of **3b, c** that rapidly interconvert by homeomorphic isomerization, and these descriptors are henceforth coupled to their alphanumeric designations. Perhaps counterintuitively, the major species have been assigned (for all macrocycle sizes) as *in,in*-**3b–e**. A strong rationale is provided in accompanying computational papers (which also show the ³¹P{¹H} NMR signals of *in* P: bridgeheads to be 3.5–8.0 ppm downfield of *out* P: bridgeheads).^{10b,20,27} As elaborated below, dispersion forces are thought to play a key role. Analogous trends were found in earlier computational studies of the hydrocarbon bicyclo[6.6.6]eicosane and related species.²⁹ However, the *in,in* thermodynamic preference is not reflected in crystal structures (*vide infra*), and of course cannot extend to smaller ring systems (*e.g.*, DABCO).

BH₃ adducts and thermal phosphorus epimerization

In principle, *in,in*-**3b–e** and *out,out*-**3b–e** could interconvert by sequential pyramidal inversions at each phosphorus atom. Although it was viewed as highly unlikely that such processes played any roles in the preceding phenomena, authentic samples of several of the potential intermediates, *in,out*-**3b–e**, were sought. If they were to be stable with respect to the *in,in* and *out,out* isomers at room temperature, their intermediacies could be definitively excluded.³⁰





Scheme 5 Conversion of title compounds to dibridgehead diphosphine diboranes.

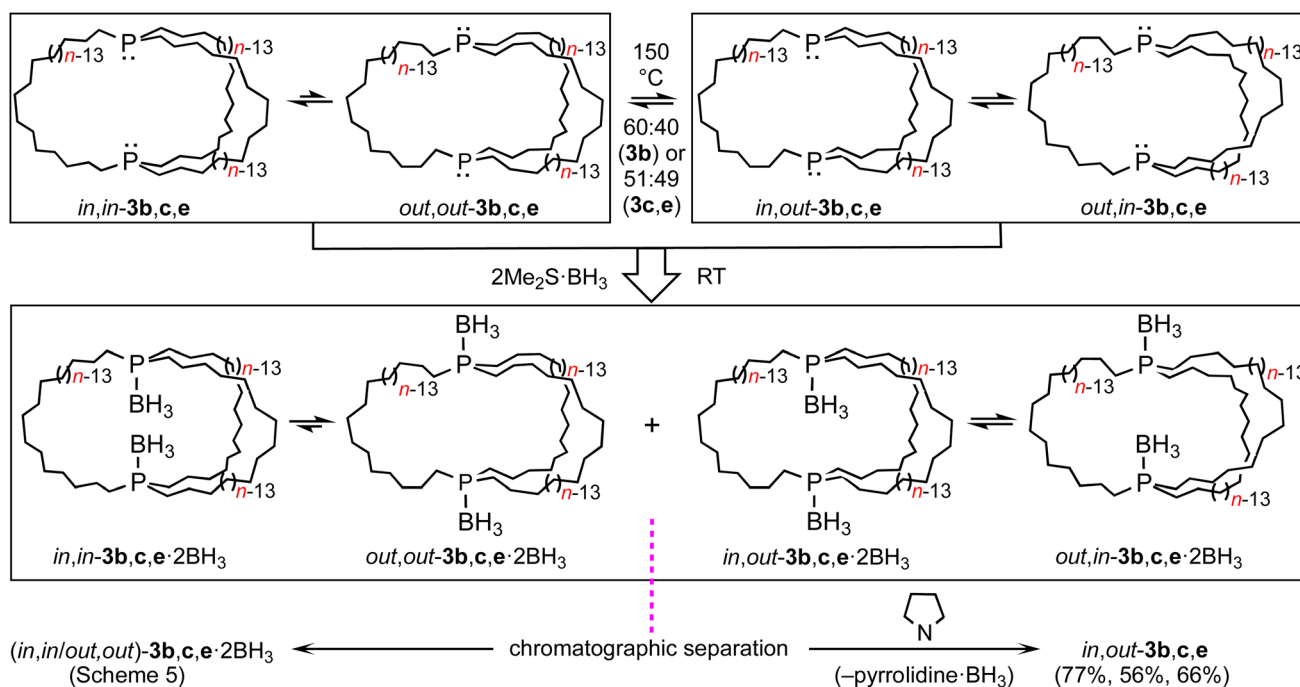
As a prelude, (*in,in/out,out*)-**3b**, **c**, **e** were treated with moderate excesses of Me₂S·BH₃. As shown in Scheme 5, workups gave the diphosphine diboranes (*in,in/out,out*)-**3b**, **c**, **e**·2BH₃ as white or light yellow analytically pure air stable solids or oils in 70–91% yields. These materials, unlike the diphosphines, can be purified chromatographically. They were characterized analogously and exhibited, like other phosphine boranes, broad boron-coupled ³¹P NMR and BH₃ ¹H NMR signals.³¹ Their isomer distributions are also of interest, but this topic is deferred to future papers.

As depicted in Scheme 6, mesitylene solutions of (*in,in/out,out*)-**3b**, **c**, **e** were kept at 150 °C and monitored by $^{31}\text{P}\{\text{H}\}$ NMR. As exemplified in Fig. S8,[†] a new signal gradually appeared in each case. These were assigned to the epimerization products *in,out*-**3b**, **c**, **e**. After 30–60 h, 60 : 40 (**3b**) to 51 : 49 (**3c**, **e**) equilibrium mixtures were obtained ((*in,in/out,out*):*in,out*). The rate of epimerization of **3c** ($k_1 = 1.47 \times 10^{-5} \text{ s}^{-1}$) gave a $\Delta G_{423 \text{ K}}^\ddagger$ value of 34.4 kcal mol $^{-1}$ ($\Delta G_{423 \text{ K}} = 0.03 \text{ kcal mol}^{-1}$), in good agreement with pyramidal inversion barriers of trialkyl monophosphines.⁸

Practical direct separations of (*in,in/out,out*)-**3b**, **c**, **e** and *in,out*-**3b**, **c**, **e** could not be devised. Thus, as shown in Scheme 6, the samples were treated with excess Me₂S·BH₃. Silica gel chromatography gave the bis(borane) adducts (*in,in/out,out*)-**3b**, **c**, **e**·2BH₃ (also prepared in Scheme 5) and *in,out*-**3b**, **c**, **e**·2BH₃ in 43–23% and 42–16% yields, respectively. The latter were characterized analogously to the former,³² and representative ¹³C{¹H} NMR spectra are compared in Fig. S9.† The phosphine boranes *in,out*-**3b**, **c**, **e**·2BH₃ were deprotected using a standard protocol, neat refluxing pyrrolidine. Silica gel workups gave analytically pure *in,out*-**3b**, **c**, **e** in 77–56% yields as moderately air sensitive colorless oils.

Additional probes of equilibria

Importantly, *in,out*-**3b**, **c**, **e** exhibited a single $^{31}\text{P}\{\text{H}\}$ NMR signal at ≥ 290 K, although by symmetry two would have been expected. This implies rapid homeomorphic isomerization (Scheme 6, upper right, or Scheme 2, lower manifold) on the



Scheme 6 Thermal epimerization of (*in,in/out,out*)-**3** to *in,out*-**3** and separations via BH₃ adducts.

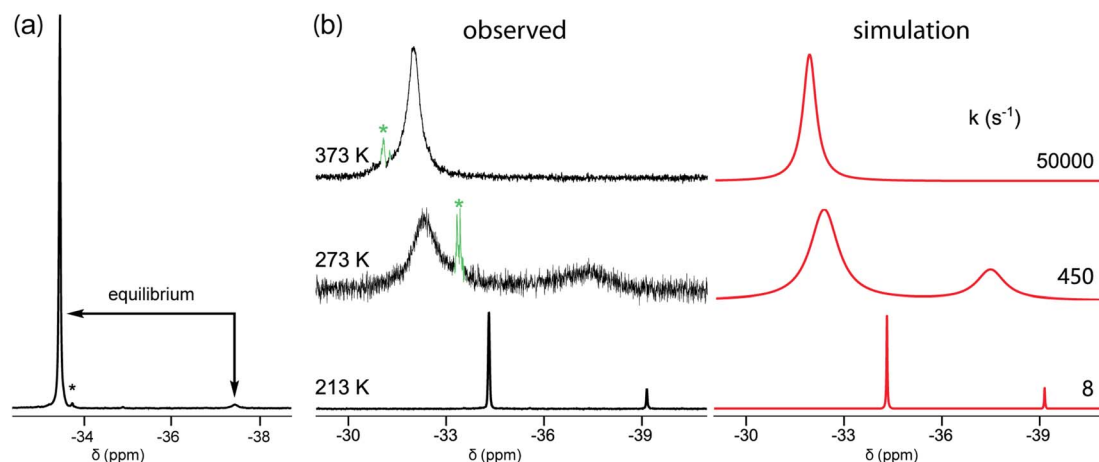


Fig. 1 $^{31}\text{P}\{^1\text{H}\}$ NMR spectra in toluene- d_8 : (a) **3c** at 193 K; (b) **3b** at 213 K, 273 K, and 373 K, together with simulated spectra. The label * indicates an impurity.

NMR time scale. Accordingly, CH_2Cl_2 solutions were cooled, and $^{31}\text{P}\{^1\text{H}\}$ NMR spectra were recorded. In the cases of *in,out*-**3b**, **c**, two signals of nearly equal intensities decoalesced as shown in Fig. 2 ($T_c = 290$ K and 200 K). The data yielded $\Delta G_{T_c}^\ddagger$ values of 12.1 and 8.5 kcal mol $^{-1}$, respectively. Thus, the

activation energies increase as the macrocycles become smaller and degrees of freedom diminish.

The chemical shifts of the decoalesced signals, and the Δppm values, were similar to those in Fig. 1. Thus, the down-field signals are provisionally assigned to *in* bridgeheads, and

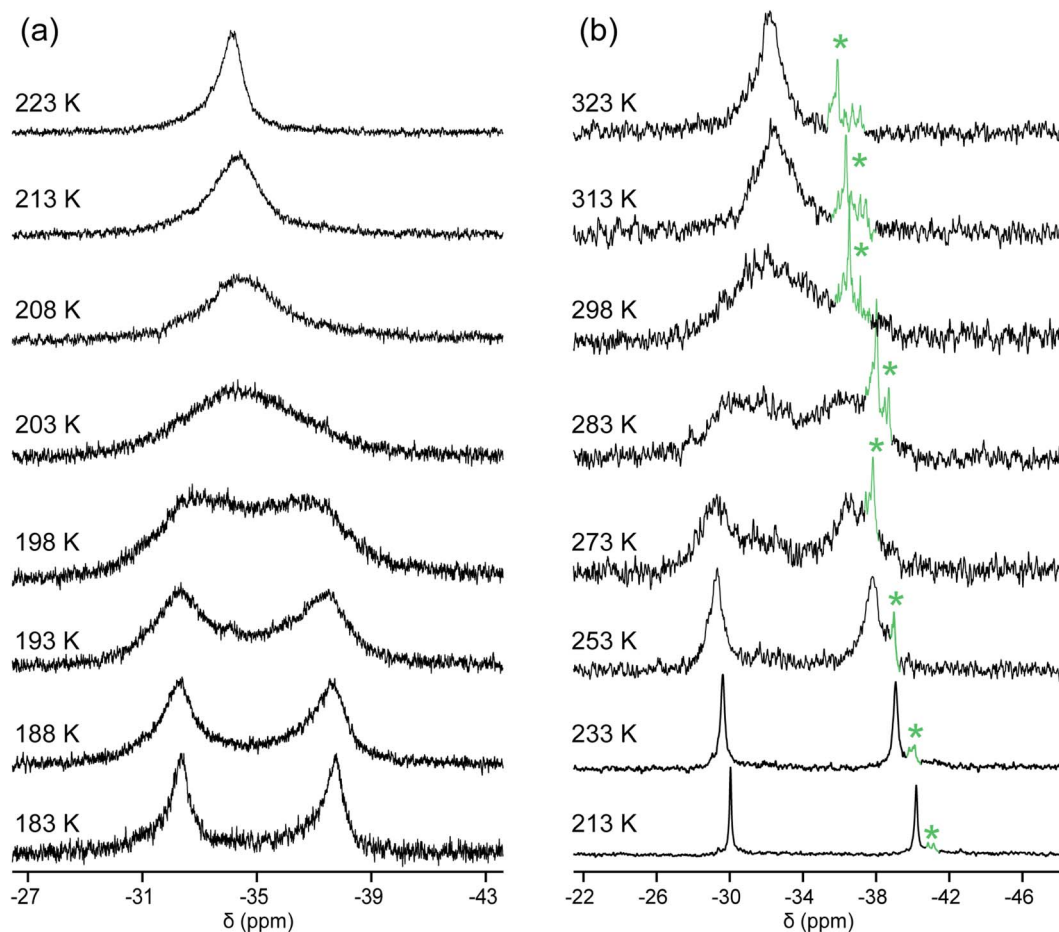


Fig. 2 Variable temperature $^{31}\text{P}\{^1\text{H}\}$ NMR spectra (202 MHz) of (a) *in,out*-**3c** in CH_2Cl_2 ; (b) *in,out*-**3b** in CDCl_3 . The label * indicates an impurity.



Table 1 Key crystallographic distances [Å] and angles [°]

	<i>out,out</i> - 3b	<i>out,out</i> - 3c	<i>out,out</i> - 3e	<i>out,out</i> - 3c ·2BH ₃ · (C ₅ H ₉ CH ₃)	<i>out,out</i> - 3c ·2BH ₃ · (C ₆ H ₁₁ CH ₃)	<i>out,out</i> - 3e ·2BH ₃ (1) ^a	<i>out,out</i> - 3e ·2BH ₃ (2) ^a	<i>out,out</i> - 3e ·2BH ₃ (3) ^a
P–P ^b	10.8271(8)	12.948(3)	17.978(1)	13.212(4)	13.220(4)	19.407(3)	19.800(3)	19.540(3)
P–C	1.8535(15)	1.8361(15)	1.848(2)	1.840(11)	1.823(8)	1.825(8)	1.827(8)	1.805(8)
	1.8544(15)			1.87(3)	1.770(11)	1.827(8)	1.817(8)	1.802(8)
	1.8526(15)		1.832(2)	1.812(8)	1.929(12)	1.801(8)	1.814(8)	1.814(9)
	1.8541(16)			1.708(13)	1.837(10)	1.825(8)	1.822(9)	1.819(8)
	1.8530(15)		1.850(2)	1.92(3)	1.738(12)	1.819(8)	1.779(10)	1.825(9)
	1.8543(15)			1.852(10)	1.825(11)	1.831(8)	1.817(9)	1.830(8)
P–B	—	—	—	1.906(12)	1.864(12)	1.903(10)	1.903(10)	1.907(10)
				1.900(12)	1.881(12)	1.903(9)	1.920(10)	1.910(10)
C–P–C	98.67(7)	98.64(6)	102.06(10)	105.9(4)	105.7(5)	107.2(4)	105.8(4)	106.9(4)
	98.68(7)			102.0(16)	102.6(5)	103.9(4)	104.4(4)	101.7(4)
	98.02(7)		100.30(11)	106(2)	107.0(5)	106.6(4)	105.7(4)	110.0(4)
	97.65(7)			101.7(5)	108.5(6)	103.7(4)	105.8(5)	107.1(4)
	99.21(7)		100.32(10)	114.4(10)	105.0(5)	109.3(4)	107.1(4)	108.2(4)
	98.11(7)			97.1(11)	102.3(5)	107.8(4)	111.3(5)	103.3(4)
C–P–B	—	—	—	117.1(6)	115.9(5)	111.5(4)	112.2(4)	110.7(4)
				109.2(15)	120.4(6)	112.7(5)	112.8(4)	116.0(4)
				114.8(5)	103.7(5)	114.4(4)	115.1(4)	111.1(4)
				118.8(7)	112.8(6)	112.8(4)	106.4(5)	112.8(5)
				109.7(10)	116.5(6)	113.2(4)	113.9(5)	109.4(5)
				112.9(6)	110.7(6)	109.6(5)	112.2(5)	114.7(4)
P–P-lone	172.9	180.0	108.5	174.2(4)	176.1(4)	149.2(3)	153.0(3)	149.2(3)
pair or P–P–B	173.5			157.6(4)	158.4(4)	133.1(3)	129.2(4)	133.3(4)
Phosphorus	295.4	295.9	302.7	313.9	315.3	317.7	315.9	318.6
pyramidalization ^c	295.0			313.2	315.8	320.8	324.2	319.2

^a The multiple columns refer to the three independent molecules in the unit cell. ^b The corresponding value in the platinum complex *trans*-**2c** is 4.61 Å. ^c Sum of the three C–P–C bond angles (360° = planar or sp² limit, 328.4° = tetrahedral or sp³ limit; 270° = unhybridized p_x/p_y/p_z limit).

the upfield signals to *out* bridgeheads. The ³¹P{¹H} NMR spectra of the diphosphine diboranes (*in,in/out,out*)-**3c**·2BH₃ and *in,out*-**3c**·2BH₃, as well as ¹H and ¹³C{¹H} NMR spectra of the latter, were recorded over a similar temperature range in CD₂Cl₂ (Fig. S10–S13†). Although the chemical shifts and peak widths varied, there were no well-defined decoalescence phenomena.

Crystal structures

Efforts were made to determine the crystal structures of as many of the preceding compounds as possible. Six were ultimately

obtained as summarized in the ESI.† Key metrical parameters are presented in Table 1, and many additional distances and angles are tabulated in the ESI.† Interestingly, all compounds exhibited *out,out* geometries. Consider first the diphosphines *out,out*-**3b**, **c**, **e**, the thermal ellipsoid plots of which are compared in Fig. 3.

Crystalline *out,out*-**3c** exhibits unusual molecular symmetry (*D*₃), such that the positions of all 44 non-hydrogen atoms can be defined from the atomic coordinates of only eight (P(CH₂)₇). As depicted in panel (a) of Fig. 4, a *C*₃ axis passes through the

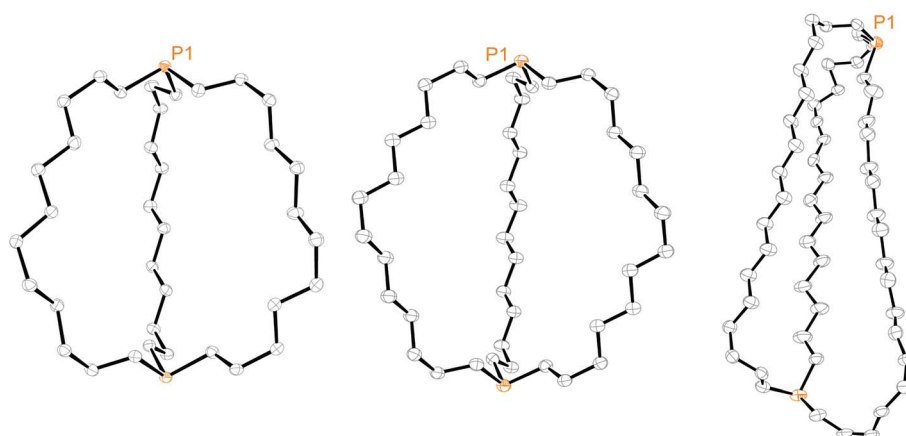


Fig. 3 Thermal ellipsoid plots (50% probability level) for *out,out*-**3b** (left), *out,out*-**3c** (middle), and *out,out*-**3e** (right, dominant conformation).



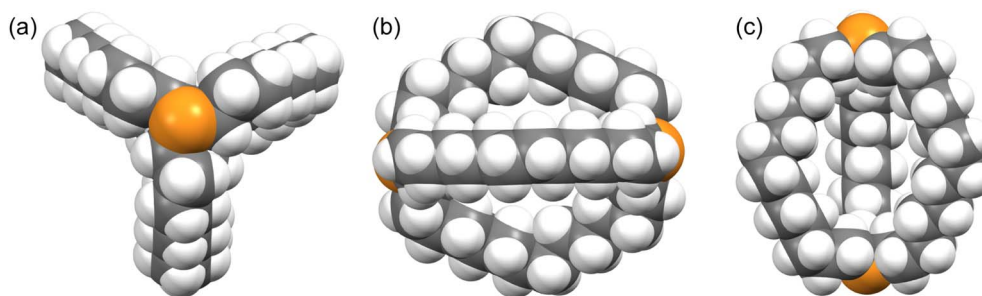


Fig. 4 Space filling representations of *out,out*-**3c** from three orthogonal perspectives.

two phosphorus atoms, and three C_2 axes lie in a perpendicular plane (one of which runs perpendicular to the plane of the paper in panel (b)). However, the conformation remains chiral, with no internal mirror planes, although as required by the achiral space group $R\bar{3}c$, both enantiomers are present in the unit cell. Panel (c) highlights the cage like nature and attendant interior space, which in the lattice is partially occupied by neighboring molecules (*vide infra*).

In the case of *out,out*-**3b**, there is a “near miss” with respect to D_3 symmetry. Space filling views comparable to those in Fig. 4 are provided in Fig. S14,[†] and visually most deviations are slight. With *out,out*-**3e** (Fig. 3), a C_2 axis passes through the midpoint of one $P(CH_2)_{18}P$ chain and exchanges the phosphorus atoms and the other two chains. As detailed in the Experimental section, there is disorder in two chains but this is easily modeled and only the dominant conformation (77%) is treated. As may be facilitated by the larger ring sizes in *out,out*-**3e**, the chains partially collapse in on each other, stopping just short of van der Waals contacts and retaining a smidgen of interior space (Fig. S15[†]). Furthermore, the two phosphorus atoms no longer occupy geometric apices.

Features associated with the phosphorus–phosphorus vectors of *out,out*-**3b**, **c**, **e** are of interest. As summarized in Table 1, their lengths increase from 10.8271(8) to 12.948(3) to 17.978(1) Å. This constitutes an immense expansion of the

phosphorus–phosphorus distances in the crystalline platinum complexes **2c**, **g** (4.611–4.620 Å), emphasizing the structural flexibility of the diphosphines. The phosphorus–phosphorus–lone pair angles in *out,out*-**3c** are both 180° , whereas in *out,out*-**3b** they decrease slightly to 173.5° – 172.9° . However, in *out,out*-**3e** the angles are both 108.5° , approaching the 90° cutoff for *out,out* and *in,in* isomers diagrammed in **II** (Scheme 1).

Consider next the diphosphine diboranes *out,out*-**3c**, **e**· $2BH_3$. The former could be crystallized as both methylcyclopentane³³ and methylcyclohexane monosolvates, *out,out*-**3c**· $2BH_3$ ·($C_5H_9CH_3$) and *out,out*-**3c**· $2BH_3$ ·($C_6H_{11}CH_3$). These exhibited very similar unit cell parameters (Table S1[†]) and molecular structures, with the solvent molecules occupying the interior of the diphosphine cages. The former (the better structure) is depicted in Fig. 5, but both are quite similar. Solvent is analogously incorporated into the diphosphine cages of crystalline digold complexes of the type *out,out*-**3c**· $2AuX$.^{11,34} The phosphorus–phosphorus vectors in *out,out*-**3c**· $2BH_3$ ·($C_5H_9CH_3$) and *out,out*-**3c**· $2BH_3$ ·($C_6H_{11}CH_3$) are 2.1% longer than that in the parent diphosphine *out,out*-**3c** (13.212(4)–13.220(4) Å vs. 12.948(3) Å), with one P–P–B angle close to 180° (174.2 – 176.1°) and the other somewhat smaller ($157.6(4)$ – $158.4(4)^\circ$).

Although *out,out*-**3e**· $2BH_3$ crystallized without solvent incorporation, three independent molecules were present in the unit cell. One has been arbitrarily selected for Fig. 5. As with the

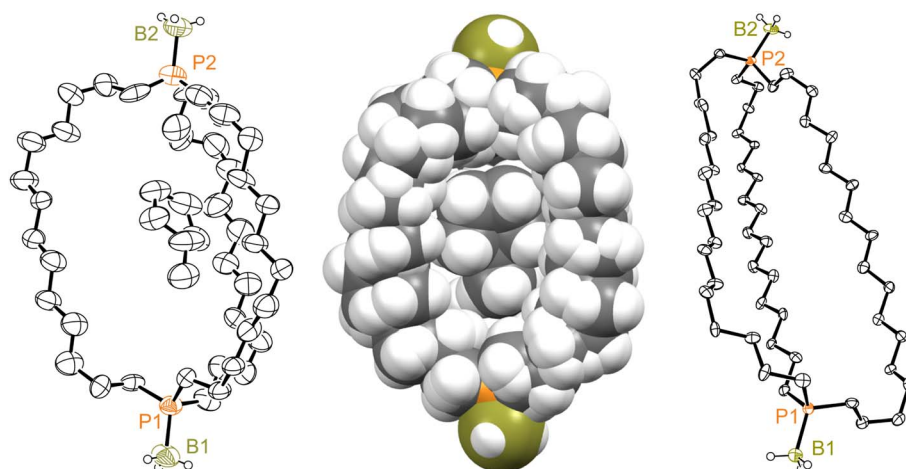


Fig. 5 Thermal ellipsoid plots (50% probability level) for *out,out*-**3c**· $2BH_3$ ·($C_5H_9CH_3$) (left, dominant conformation) and *out,out*-**3e**· $2BH_3$ (right, one of three independent molecules in the unit cell), and a space filling representation of *out,out*-**3c**· $2BH_3$ ·($C_5H_9CH_3$) (middle).



congener *out,out*-**3e**, the cages in all three molecules have collapsed inward, with the $\text{P}(\text{CH}_2)_{18}\text{P}$ chains close to but not quite in van der Waals contact. As expected, the phosphorus–phosphorus vectors (19.407(3)–19.800(3) Å) are much longer than those of the *out,out*-**3c**· 2BH_3 monosolvates, and for conformational reasons longer than that in *out,out*-**3e** (17.978(1) Å). The P–P–B angles (153.0(3)–129.2(4)°; avg 141.2°) are smaller than the P–P–(B or lone pair) angles of all the compounds except *out,out*-**3e** (108.5°).

Crystal lattices

The unexpected uniformity with which the preceding compounds crystallized as *out,out* isomers prompted close inspections of the crystal lattices for potential “packing forces”. The crystal systems exhibited by *out,out*-**3b**, **c**, **e** (triclinic, rhombohedral, monoclinic; $Z = 2, 6, 4$) differed. However, the unit cells always featured one axis that was very much longer than the others (Table S1†), as particularly pronounced for *out,out*-**3c** ($c = 89.58(2)$ Å vs. $2 \times 9.1903(19)$ Å). When viewed along this axis, the phosphorus–phosphorus vectors are aligned, as highlighted in orange in panel (a) of Fig. 6. Each stack is surrounded by six others, all equidistant and in a hexagon motif.

There are six $(\text{CH}_2)_{14}$ segments radiating with 60° spacings from each phosphorus–phosphorus stack, the PCH_2 segments of which generate apparent rhomboids, followed by “tails”

representing the remaining CH_2 groups. Three are associated with one layer of molecules aligned along the c axis, and the other three with a layer that is three layers above or below (Fig. 6, panel (b)). Within each layer, the $(\text{CH}_2)_{14}$ bridge of one molecule intercalates between two $(\text{CH}_2)_{14}$ bridges of a neighboring molecule (panel (c)). Between adjacent layers, the molecules are offset, the phosphorus atoms of one abutting the $\text{PCH}_2\text{CH}_2\text{CH}_2$ groups of the other. However, the closest intermolecular distances fall just short of van der Waals contacts.

Although *out,out*-**3b** does not give as symmetrical a lattice as *out,out*-**3c**, the $(\text{CH}_2)_{12}$ chains similarly nest within the interstices generated by two $(\text{CH}_2)_{12}$ chains of a neighboring molecule (Fig. 7). The two bis(borane) adducts *out,out*-**3c**· 2BH_3 · $(\text{C}_5\text{H}_9\text{CH}_3)$ and *out,out*-**3c**· 2BH_3 · $(\text{C}_6\text{H}_{11}\text{CH}_3)$ pack similarly. Here, the interior solvent molecules require expression as *out,out* isomers, so crystal packing forces cannot be playing a direct role.

The long dimensions of the $\text{P}(\text{CH}_2)_{18}\text{P}$ systems *out,out*-**3e** and *out,out*-**3e**· 2BH_3 are also roughly aligned in the respective crystal lattices. However, as illustrated in Fig. 8, there is no intercalation as in Fig. 6. Nonetheless, the intermolecular spacings between $(\text{CH}_2)_{18}$ chains are comparable to the intramolecular spacings, which as noted above are slightly greater than van der Waals contacts. Interestingly, *out,out*-**3e** and *out,out*-**3e**· 2BH_3 exhibit the highest densities in each series (e.g., ρ 1.022 (*out,out*-**3e**) vs. 0.991–0.990 (*out,out*-**3b**, **c**) Mg m^{-3}).

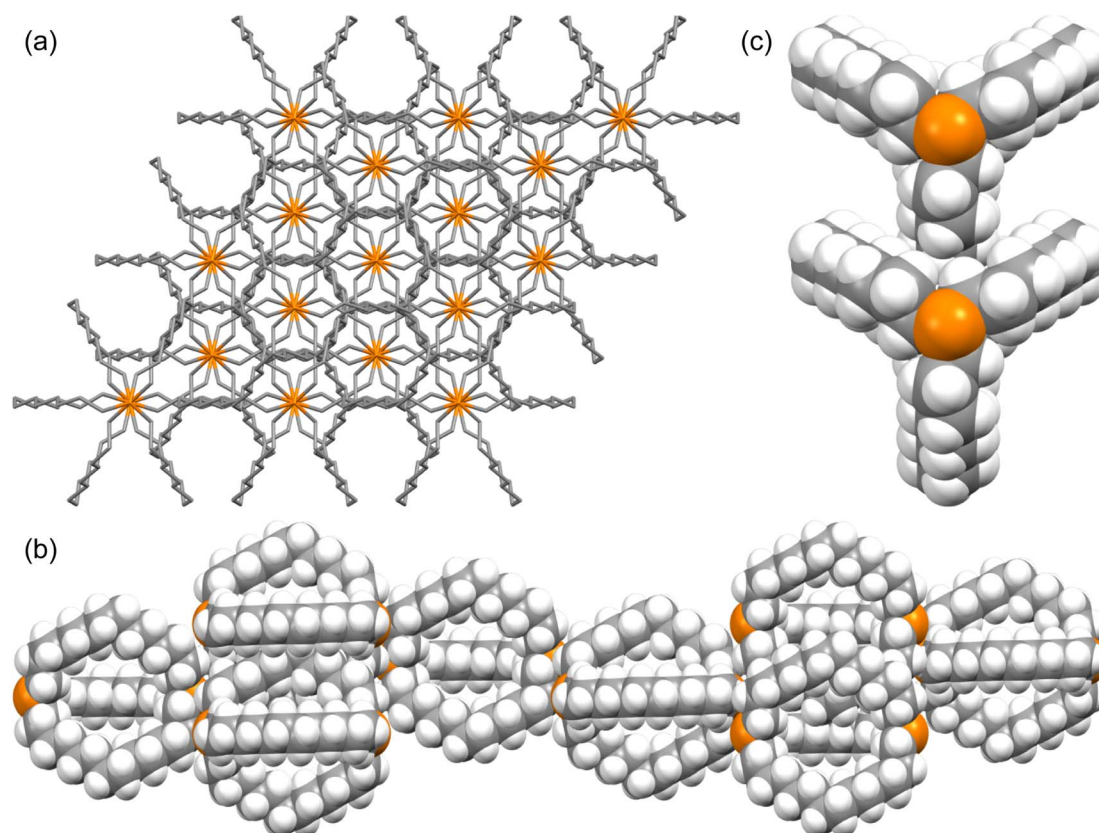


Fig. 6 Views of the crystal lattice of *out,out*-**3c** with the long c axis perpendicular to the plane of the paper (a and c) or in the plane of the paper (b).



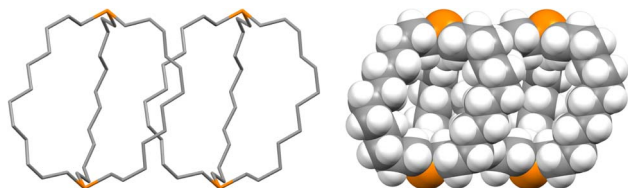


Fig. 7 Two adjacent molecules in the crystal lattice of *out,out*-3b.

Discussion

Syntheses of dibridgehead diphosphines

As shown in Scheme 3, this study has established the synthetic availability of an extensive family of aliphatic macrocyclic dibridgehead diphosphines $P((CH_2)_n)_3P$ (3) that can exist as *in,in*, *out,out*, and *in,out* isomers. There currently seems to be no obstacle to extending this chemistry to $n \geq 20$, or ≥ 42 membered macrocycles. As depicted in Scheme 7 (top), isomers of 3c ($n = 14$) have also been accessed *via* three-fold intermolecular olefin metatheses of the metal-free phosphine borane $H_3B \cdot P((CH_2)_6CH=CH_2)_3$.³² However, the metathesis steps proceed in much lower yields than the platinum templated pathway, and the overall yields are miniscule.

As exemplified by 6c in Scheme 7 (bottom), demetallation of gyroscope-like rhodium(i) complexes can also be effected,³⁵ but in efforts to date yields have not been superior to the routes in Scheme 3. Precursors such as 7 afford related dibridgehead di(triaryl)phosphines.^{35b} However, there have recently been promising developments regarding alternative routes that involve inexpensive metals.²⁸ These have included the iron-based syntheses of the dibridgehead diarsines $As((CH_2)_n)_3As$ ($n = 10, 12, 14$).³⁶

The mechanisms of these demetalations, which are receiving ongoing attention, are beyond the scope of this study. However, since metal fragments can generally be reintroduced (Scheme

4), intermediates such as **X** (Scheme 7) derived from metal-phosphorus bond cleavage and homeomorphic isomerization have been suggested. The platinum byproducts $M_2Pt(C\equiv X)_4$ generated in Scheme 3 would be derived from the displacement of all the metal-ligand bonds in **X** by $-C\equiv X$ nucleophiles. Accordingly, excess $KC\equiv N$ has been shown to convert various *cis*- $PtCl_2$ (diphosphine) adducts to $K_2Pt(C\equiv N)_4$.²³

The most closely related dibridgehead diphosphorus macrocycles in the literature are depicted in Scheme 8.^{17b} The dibridgehead di(triaryl)phosphine dioxides **8·2O** were constructed *via* Williamson ether syntheses that afforded both (*in,in/out,out*) and *in,out* isomers. Subsequent reductions gave **8**, which were characterized *in situ* due to their air sensitivity. It has not yet proved possible to quantify equilibrium ratios or obtain crystal structures for any of these species. Nonetheless, the *in/out* isomers could be assigned based upon rate trends in Scheme 8 and derivatization reactions. Recently, several additional types of novel compounds exhibiting *in/out* isomerism have been reported.^{15,37}

Isomer assignments

In certain cases, unequivocal isomer assignments are possible for the preceding compounds. For example, the thermal epimerisation of **3b**, **c**, **e** in Scheme 4 give species that can exhibit two $^{31}P\{^1H\}$ NMR signals of equal areas at low temperatures. These can only be *in,out* isomers that undergo rapid homeomorphic isomerization. The other isomers must therefore represent the *in,in/out,out* manifold as mapped in Scheme 2. Similarly, there are two cases in which the *in,in/out,out* isomers exhibit two $^{31}P\{^1H\}$ NMR signals (unequal areas) at low temperature. One of these must represent an *in,in* isomer, and the other *out,out*. Our rationale for assigning the dominant isomer as *in,in*, which is perhaps counterintuitive, is as follows.

First, the earliest computational probes of such equilibria, conducted with the hydrocarbons $HC((CH_2)_n)_3CH$, pointed to

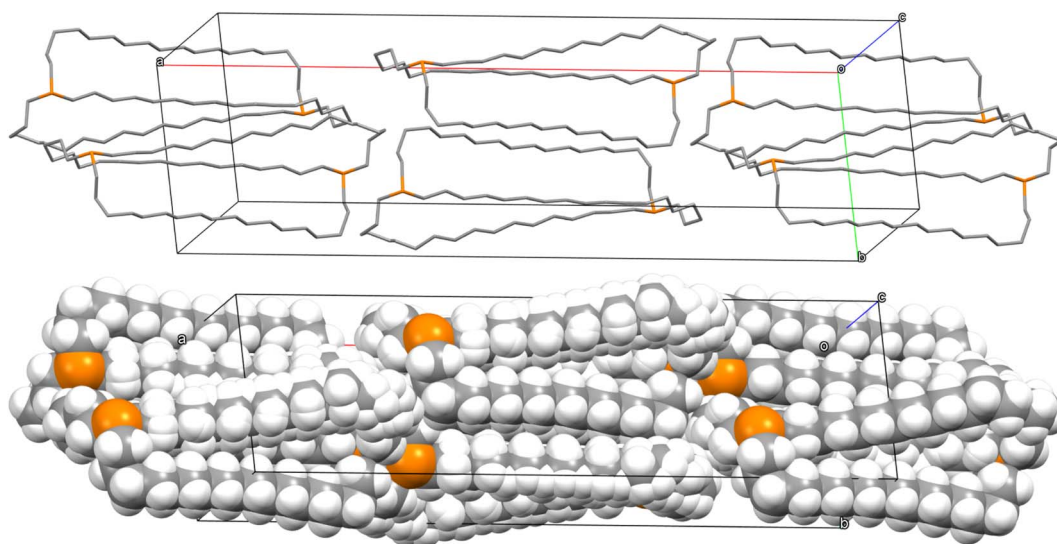
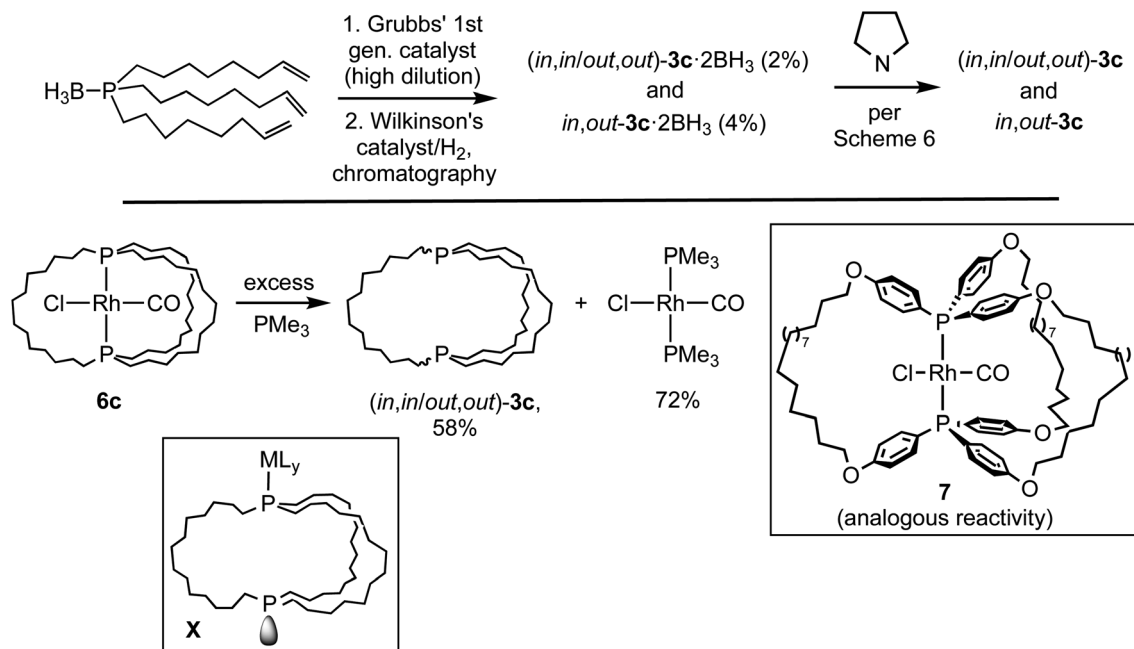


Fig. 8 Adjacent molecules in the crystal lattice of *out,out*-3e (dominant conformations only).

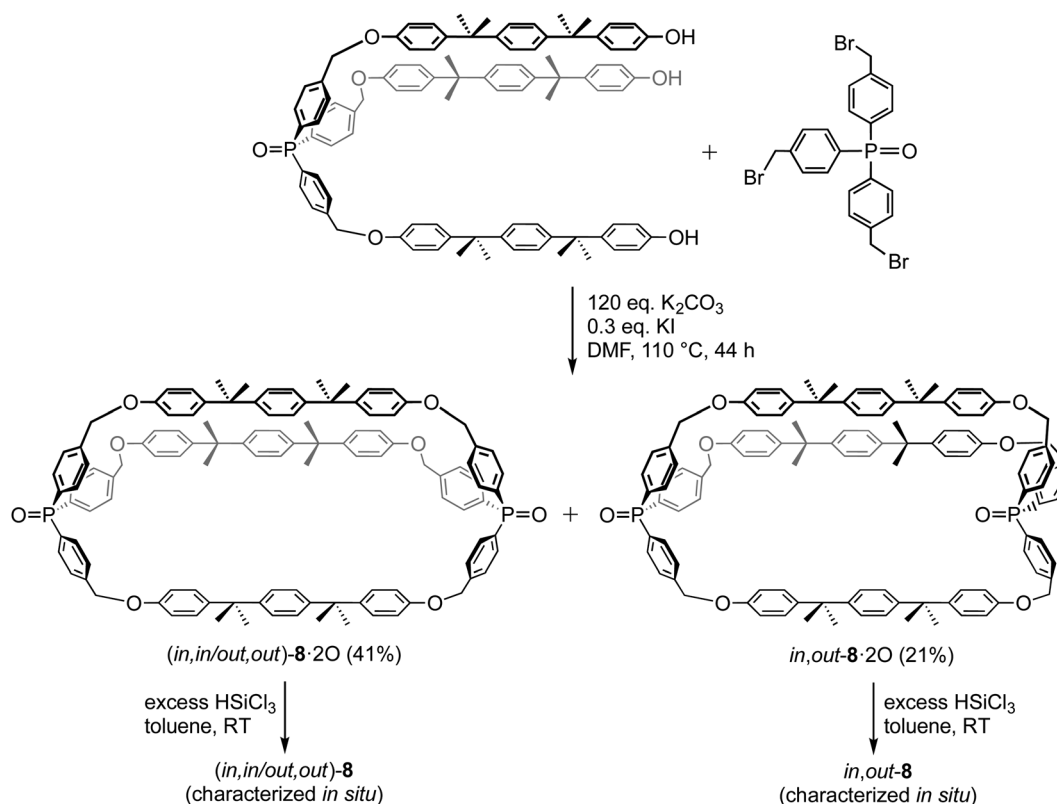




Scheme 7 Additional routes to the title molecules and related species.

an increasing and eventually dominant proportion of *in,in* isomers as *n* is increased.²⁹ Second, DFT calculations with $(P(CH_2)_n)_3P$ ($n = 8-20$) have always given parallel results.^{10,21} As reported separately, DFT has also been used to compute the ³¹P

NMR chemical shifts ($n = 10-20$),^{10b,20} and two relationships emerge: (1) the chemical shifts of the *in,in* isomers are downfield of the *out,out* isomers, and (2) the chemical shifts of the *in* bridgeheads of the *in,out* isomers are downfield of the *out*

Scheme 8 Macrocyclic dibridgehead diphosphorus compounds reported by Bauer.^{17b}

bridgeheads (Δppm similar to experiment in both cases).²⁷ Inverting the assignments made above would contradict these findings.

Molecular dynamics simulations have also been carried out.¹⁰ These indicate an abundance of conformers that are relatively closely spaced in energy for all limiting isomers. Several factors point to increased attractive intramolecular dispersion (van der Waals) forces in the *in,in* as opposed to *out,out* isomers. For example, a reduced surface area should translate into a reduced void space in these cage-like structures. The latter should in turn increase the dispersive (attractive) van der Waals forces between methylene linkers. Accordingly, the Connolly contact surfaces³⁸ generated using various probe radii (e.g., 4.0 Å, comparable to a small solvent molecule) are on the average lower for the ensemble of low-energy conformations for the *in,in* isomers. We note in passing that additional computational studies have addressed other aspects of *in/out* isomerism.^{12,15,37}

Further analyses of equilibria and dynamic properties

The *in,in* and *out,out* equilibrium ratios for **3b**, **c**, 86 : 14 and 97 : 3 (213 K and 193 K, toluene- d_8), correspond to small ΔG values (0.77, 1.33 kcal mol⁻¹) at the temperatures of measurement. Importantly, the proportion of *out,out* isomer increases in the smaller macrocycle,²⁷ as would be expected as a limiting bicyclo [2.2.2]octane-based structure such as DABCO is approached. The equilibrium ratios of (*in,in/out,out*)-**3b**, **c**, **e** versus *in,out*-**3b**, **c**, **e**, as established at 150 °C (Scheme 6), are not very dependent upon the macrocycle size. The slightly greater bias of **3b** towards the (*in,in/out,out*)-isomers (60 : 40 vs. 51 : 49) is consistent with a small decrease in the relative stabilities of *in,out* isomers with decreasing ring sizes.

The ΔG^\ddagger values for the homeomorphic isomerization of *out,out*-**3** to *in,in*-**3** increase as the ring sizes decrease (10.4 kcal mol⁻¹ for **3c**, 193 K vs. 11.4 kcal mol⁻¹ for **3b**, 213 K). Importantly, the ΔS^\ddagger values become more negative as the ring sizes decrease (−11.8 eu, **3c**; −19.4 eu, **3b**). This is consistent with a more pronounced loss of degrees of freedom in turning the smaller macrocycle inside out. However, the ΔH^\ddagger values decrease (8.2 kcal mol⁻¹, **3c**; 7.3 kcal mol⁻¹, **3b**), hinting at a possible isokinetic relationship.³⁹ Interestingly, the ΔG^\ddagger value for the degenerate homeomorphic isomerization of *in,out*-**3c** (8.5 kcal mol⁻¹, 200 K) is less than those for the non-degenerate isomerizations of *in,in*-**3c** and *out,out*-**3c** (10.4 or 11.5 kcal mol⁻¹, 193 K, depending upon direction). The trend for *in,out*-**3b** compared to *in,in*- and *out,out*-**3b** is analogous but less pronounced (290 K: 12.1 vs. 13.1 or 13.8 kcal mol⁻¹).

The epimerisations of (*in,in/out,out*)-**3b**, **c**, **e** (Scheme 6) require similar temperatures and time scales. As noted above, the ΔG^\ddagger value for (*in,in/out,out*)-**3c** (34.4 kcal mol⁻¹, 150 °C or 423 K) is typical for inversions of acyclic trialkylphosphines. This suggests a common bridgehead inversion mechanism, as opposed to unconventional pathways involving phosphorus–phosphorus interactions that could show a dependency upon macrocycle size. Reactions of dibridgehead diphosphines with $\text{P}(\text{CH}_2)_n\text{P}$ linkages with $n \leq 4$ can afford species with

phosphorus–phosphorus bonds, for which inversions at phosphorus have been documented.⁴⁰

Of course, all the same questions can be posed with regard to the diphosphine diboranes $3 \cdot 2\text{BH}_3$. These are beyond the scope of this paper, but it is clear that equilibria involving *in,in* and *out,out* isomers, or degenerate *in,out* species, remain rapid on NMR time scales. Despite the greater steric demand of a bridgehead BH_3 substituent as opposed to a lone pair, we believe that the diphosphines in this study provide ample clearance for *in,in* and *in,out* isomers. However, when the BH_3 groups of *in,out*-**3c** $\cdot 2\text{BH}_3$ are replaced by bulky gold(i) Lewis acids AuAr as in **9** (Scheme 9), steric interactions greatly increase. Accordingly, the structure “flips” into an *out,out* form with crossed chains (see **VIII**, Scheme 2), both in solution and the solid state.¹¹

Finally, it should be kept in mind that a wide variety of mechanisms may be operative in *in/out* isomerizations. For example, dibridgehead diorthoesters with $(\text{OCH}_2\text{CH}_2)_n$ bridges have recently been prepared, as exemplified by **10** in Scheme 9.¹⁵ All three *in/out* orientations of the $\text{HC}(\text{OR})_3$ units can be observed. These can equilibrate by both homeomorphic isomerizations and catalyzed pathways involving cleavage of the carbon–oxygen bonds.

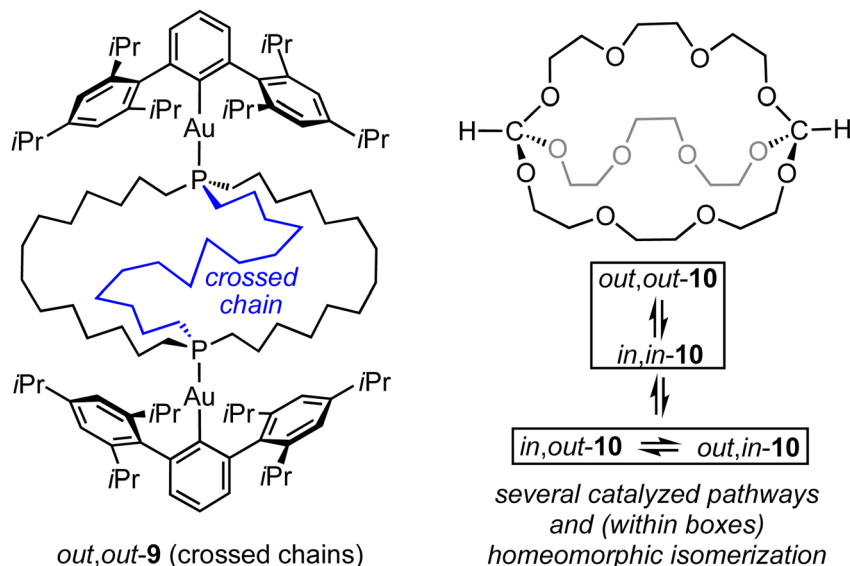
Crystal structures

As shown in Fig. 3, the dibridgehead diphosphines **3b**, **c**, **e** all crystallize as *out,out* isomers, despite the conclusions in the preceding sections that *in,in* isomers dominate in solution. There are many cases where a compound crystallizes as the less stable of two possible isomers, which is commonly attributed to packing forces. However, this is rarely observed for an entire series of compounds. In the case of *out,out*-**3c**, Fig. 6 convincingly documents a highly symmetric molecular structure (D_3) that affords an exceptional lattice with optimal intermolecular contacts as analyzed above. The dibridgehead diarsine $\text{As}((\text{CH}_2)_{14})_3\text{As}$ crystallizes analogously.⁴¹

Crystalline *out,out*-**3b** as well as the arsenic homolog $\text{As}((\text{CH}_2)_{12})_3\text{As}$ ³⁶ are just a few CH_2 – CH_2 rotations removed from D_3 symmetry, and share several packing features with *out,out*-**3c** (e.g., Fig. 7). As shown in Fig. 8, *out,out*-**3e** crystallizes in a much different motif, but still with a visually impressive degree of van der Waals contacts or near-contacts. In any event, these apparently trump the greater intramolecular dispersion forces posited for individual *in,in* isomers. Nonetheless, this dichotomy remains an obvious focus for further study and interpretation.

The bridgehead phosphorus atoms in *out,out*-**3b**, **c**, **e** are much more pyramidalized than in *out,out*-**3c**, **e** $\cdot 2\text{BH}_3$, as evidenced by the sums of the three carbon–phosphorus–carbon bond angles (295.0–302.7° vs. 313.2–324.3°; Table 1). The solvent occupied cages in the two structures of *out,out*-**3c** $\cdot 2\text{BH}_3$ raise the issue of whether any of the equilibria or other phenomena described above might be affected by encapsulated solvent. We view the solvate molecules as simple consequences of crystal growth, as our gyroscope-like complexes (e.g., *trans*-**2g** in Scheme 3)^{18b} occasionally but by no means routinely



Scheme 9 Additional types of compounds exhibiting *in/out* isomerism.

crystallize with a solvent molecule within a macrocycle.³⁴ Also, attempts to detect toluene-*d*_n adducts of *in,in-3c* or *out,out-3c* at low temperatures in CD₂Cl₂ and other solvents have been unsuccessful.

Conclusion

This study has brought heretofore unavailable definition to equilibria and dynamic and configurational processes involving the most fundamental type of large-ring aliphatic bicyclic compounds with bridgehead heteroatoms, XE((CH₂)_n)₃EX. The new dibridgehead diphosphines **3b–e** are highly flexible with extensive manifolds of conformations and coordination modes. They represent very promising building blocks for both mono-metallic and poly-metallic or polymeric systems – research directions that will be facilitated as improved syntheses are developed.²⁸ Monometallic adducts of *in,in* isomers have been termed gyroscope-like and are attractive springboards for molecular gyroscopes.⁴² The dynamic properties of **3c**, **e** have already been put to use in metal transport protocols,⁵ and all of the preceding directions of inquiry are actively being extended to diarsine^{36,41} and phosphine oxide analogs (EX = As, PO).¹³ These and related themes will be the subject of future reports from this laboratory.

Experimental section

(in,in/out,out)-P((CH₂)₁₂)₃P ((in,in/out,out)-3b)

A Schlenk flask was charged with *cis*-PtCl₂(P((CH₂)₁₂)₃)₂ (*cis-2b*;¹⁹ 0.1010 g, 0.1213 mmol), KCN (0.097 g, 1.489 mmol), THF (15 mL) and degassed water (0.5 mL). The mixture was stirred (24 h). The solvent was removed from the filtrate by oil pump vacuum. The residue was filtered through a pad of silica (1.5 × 1 cm). The filter cake was washed with CH₂Cl₂ (2 × 10 mL). The

solvent was removed from the filtrate by oil pump vacuum to give *(in,in/out,out)-3b* (0.0488 g, 0.0861 mmol, 71%) as a white solid, mp 52–55 °C. Anal. calcd for C₃₆H₇₂P₂ (566.90): C, 76.27; H, 12.80; found: C, 76.49; H, 12.82.

NMR (CDCl₃, δ/ppm): ¹H (500 MHz) 1.46–1.35, 1.35–1.25 (2 br m, 72H, CH₂); ¹³C{¹H} (126 MHz) 30.9 (d, *J*_{CP} = 9.5 Hz, CH₂), 28.5 (s, CH₂), 28.4 (s, CH₂), 28.1 (s, CH₂), 26.3–25.9 (br s, CH₂), 25.0–24.7 (br s, CH₂); ³¹P{¹H} (202 MHz) –29.7 to –32.1 (br s).

NMR (toluene-*d*₈, δ/ppm, 373 K): ¹H (500 MHz) 1.45–1.35, 1.35–1.23 (2 br m, 72H, CH₂); ¹³C{¹H} (126 MHz) 30.8 (d, *J*_{CP} = 10.1 Hz, CH₂), 28.71 (s, CH₂), 28.70 (s, CH₂), 28.67 (s, CH₂), 28.3 (d, *J*_{CP} = 14.6 Hz, CH₂), 26.0 (d, *J*_{CP} = 13.4 Hz, CH₂); ³¹P{¹H} (202 MHz) –31.9 (br s).

(in,in/out,out)-P((CH₂)₁₄)₃P ((in,in/out,out)-3c)

A Schlenk flask was charged with *trans*-PtCl₂(P((CH₂)₁₄)₃)₂ (*trans-2c*;^{18a} 0.4356 g, 0.475 mmol), KCN (0.4674 g, 7.177 mmol), THF (20 mL) and degassed water (0.5 mL). The mixture was stirred (24 h) and filtered to remove a yellow precipitate. The solvent was removed from the filtrate by oil pump vacuum to give *in,in/out,out-3c* (0.2692 g, 0.411 mmol, 87%) as a white solid, mp 68 °C. Anal. calcd for C₄₂H₈₄P₂ (651.06): C, 77.48; H, 13.00; found: C, 77.67; H, 13.08.

NMR (CDCl₃, δ/ppm): ¹H (500 MHz) 1.37–1.32, 1.31–1.23 (2 br m, 84H, CH₂); ¹³C{¹H} (126 MHz) 31.2 (d, *J*_{CP} = 10.3 Hz, CH₂), 29.2 (s, CH₂), 29.14 (s, CH₂), 29.08 (s, CH₂), 28.7 (s, CH₂), 26.3 (d, *J*_{CP} = 12.2 Hz, CH₂), 25.2 (d, *J*_{CP} = 11.0 Hz, CH₂); ³¹P{¹H} (202 MHz) –30.1 (s).

A ¹³C{¹H} NMR spectrum of the yellow precipitate showed signals (D₂O, δ/ppm) for K₂Pt(CN)₄ (126.5; lit⁴³ 126.5) and KCN (166.8). The precipitate was dissolved in water (5 mL) and the solution allowed to slowly concentrate. After 7 d, thin colorless plates of K₂Pt(CN)₄ were obtained, as verified by X-ray crystallography.⁴⁴



(*in,in/out,out*)-P((CH₂)₁₆)₃P ((*in,in/out,out*)-3d)

A Schlenk flask was charged with *cis*-PtCl₂(P((CH₂)₁₆)₃)₂ (*cis*-2d;¹⁹ 0.2453 g, 0.245 mmol), KCN (0.2393 g, 3.675 mmol), THF (15 mL), and degassed water (0.5 mL). The mixture was stirred. After 24 h, the mixture was filtered. The filter cake was washed with THF (2 × 5 mL). The solvent was removed from the filtrate by oil pump vacuum, and CH₂Cl₂ (25 mL) added to the solid residue. The sample was filtered through a pad of silica (1.5 × 1 cm). The filter cake was washed with CH₂Cl₂ (2 × 10 mL). The solvent was removed from the filtrate by oil pump vacuum to give (*in,in/out,out*)-3d (0.1476 g, 0.201 mmol, 82%) as a white solid, mp 56–59 °C.

NMR (CDCl₃, δ/ppm): ¹H (500 MHz) 1.46–1.33, 1.33–1.23 (2 br m, 96H, CH₂); ¹³C{¹H} (126 MHz) 31.2 (d, J_{CP} = 10.2 Hz, CH₂), 29.2 (s, 2 × CH₂), 29.1 (s, CH₂), 29.0 (s, CH₂), 28.8 (s, CH₂), 26.6 (d, J_{CP} = 12.0 Hz, CH₂), 25.4 (d, J_{CP} = 11.6 Hz, CH₂); ³¹P{¹H} (202 MHz) –30.7 (s).

(*in,in/out,out*)-P((CH₂)₁₈)₃P ((*in,in/out,out*)-3e)

A Schlenk flask was charged with *trans*-PtCl₂(P((CH₂)₁₈)₃)₂ (*trans*-2e;¹⁸ 0.2529 g, 0.233 mmol), KCN (0.2319 g, 3.561 mmol), THF (15 mL), and degassed water (0.5 mL) with stirring. After 24 h, the mixture was filtered. The filter cake was washed with THF (2 × 5 mL). The solvent was removed from the filtrate by oil pump vacuum, and CH₂Cl₂ (25 mL) added to the solid residue. The sample was filtered through a pad of silica (1.5 × 1 cm). The filter cake was washed with CH₂Cl₂ (2 × 10 mL). The solvent was removed from the filtrate by oil pump vacuum to give (*in,in/out,out*)-3e (0.1622 g, 0.198 mmol, 85%) as a white solid, mp 54–57 °C. Anal. calcd for C₅₄H₁₀₈P₂ (819.38): C, 79.15; H, 13.29; found: C, 79.16; H, 13.48.

NMR (C₆D₆, δ/ppm): ¹H (500 MHz) 1.60–1.52 (br m, 12H, CH₂), 1.49–1.40 (br m, 24H, CH₂), 1.40–1.29 (br m, 72H, CH₂); ¹³C{¹H} (126 MHz) 32.1 (d, J_{CP} = 10.5 Hz, CH₂), 30.34 (s, CH₂), 30.32 (s, CH₂), 30.3 (s, CH₂), 30.2 (s, CH₂), 30.1 (s, CH₂), 30.0 (s, CH₂), 28.4 (d, J_{CP} = 13.6 Hz, CH₂), 26.8 (d, J_{CP} = 13.0 Hz, CH₂); ³¹P{¹H} (202 MHz) –32.8 (s). IR (cm^{−1}, powder film): 2916 (s), 2847 (s), 1466 (s), 1442 (s), 725 (s).

(*in,in/out,out*)-3b·2BH₃

A Schlenk flask was charged with (*in,in/out,out*)-3b (0.0705 g, 0.124 mmol) and THF (10 mL). Then Me₂S·BH₃ (2.0 M in THF; 0.13 mL, 0.26 mmol) was added with stirring. After 1 d, the solvent was removed by oil pump vacuum. The residue was chromatographed on a silica column (4 × 30 cm) using hexanes/CH₂Cl₂ (1 : 2 v/v). The solvents were removed from the product fractions by oil pump vacuum to give (*in,in/out,out*)-3b·2BH₃ (0.0521 g, 0.0876 mmol, 70%) as a light yellow oil. Anal. calcd for C₃₆H₇₈B₂P₂ (594.57): C, 72.72; H, 13.22; found: C, 72.72; H, 13.01.

NMR (CDCl₃, δ/ppm): ¹H (500 MHz) 1.63–1.53 (m, 12H, CH₂), 1.53–1.44 (m, 12H, CH₂), 1.41–1.37 (m, 12H, CH₂), 1.37–1.23 (m, 36H, CH₂), 0.48 and 0.27 (br apparent d, 6H, BH₃); ¹³C{¹H} (126 MHz) 30.3 (d, J_{CP} = 11.9 Hz, CH₂), 28.9 (s, CH₂), 28.5 (s, CH₂),

28.1 (s, CH₂), 22.4 (d, J_{CP} = 34.0 Hz, CH₂), 21.9 (d, J_{CP} = 2.9 Hz, CH₂); ³¹P{¹H} (202 MHz): 15.0–13.7 (br s).^{31b}

(*in,in/out,out*)-3c·2BH₃

A J. Young NMR tube was charged with *in,in/out,out*-3c (0.0271 g, 0.0416 mmol), CDCl₃ (0.6 mL), and Me₂S·BH₃ (0.20 mL, 2.0 M in THF, 0.40 mmol). After 1 d, the solvent was removed *in vacuo*. The residue was passed through silica gel (1 × 15 cm) using hexanes/CH₂Cl₂ (2 : 1 v/v). The solvent was removed *in vacuo* to give *in,in/out,out*-3c·2BH₃ (0.0211 g, 0.0311 mmol, 75%) as a white solid, mp 112 °C. DSC (T_i/T_e/T_p/T_c/T_f): 95.8/110.6/112.7/114.2/117.5 °C (endotherm). TGA: onset of mass loss, 282 °C. Anal. calcd for C₄₂H₉₀B₂P₂ (678.73): C, 74.32; H, 13.37; found C, 74.01; H, 13.08.

NMR (CDCl₃, δ/ppm): ¹H (500 MHz) 1.60–1.49 (m, 12H, CH₂), 1.50–1.41 (m, 12H, CH₂), 1.41–1.32 (m, 12H, CH₂), 1.32–1.20 (m, 48H, CH₂), 0.38 and 0.26 (br apparent d, 6H, BH₃); ¹³C{¹H} (126 MHz) 30.7 (d, J_{CP} = 12.1 Hz, CH₂), 29.31 (s, CH₂), 29.25 (s, CH₂), 29.0 (s, CH₂), 28.5 (s, CH₂), 22.5 (d, J_{CP} = 34.1 Hz, CH₂), 22.2 (d, J_{CP} = 2.6 Hz, CH₂); ³¹P{¹H} (202 MHz) 16.2–14.4 (br s).^{31b} IR (cm^{−1}, powder film): 2922 (s), 2853 (s), 2366 (m), 1467 (w), 1061 (m), 718 (m). MS (EI): 678 (M⁺, 1%), 665 ([M – BH₃]⁺, 38%), 651 ([M – 2BH₃]⁺, 100%).

(*in,in/out,out*)-3e·2BH₃

A Schlenk flask was charged with (*in,in/out,out*)-3e (0.2147 g, 0.262 mmol) and THF (15 mL). Then Me₂S·BH₃ (2.0 M in THF; 0.65 mL, 1.3 mmol) was added with stirring. After 1 d, the solvent was removed by oil pump vacuum. The residue was chromatographed on a silica column (4 × 46 cm) using hexanes/CH₂Cl₂ (1 : 0 to 0 : 1 v/v). The solvents were removed from the product fractions by oil pump vacuum to give (*in,in/out,out*)-3e·2BH₃ (0.2027 g, 0.239 mmol, 91%) as a white powder, mp 67–69 °C. Anal. calcd for C₅₄H₁₁₄P₂B₂ (847.07): C, 76.57; H, 13.57; found: C, 76.28; H, 13.62.

NMR (CDCl₃, δ/ppm): ¹H (500 MHz): 1.60–1.52 (m, 12H, CH₂), 1.52–1.42 (m, 12H, CH₂), 1.42–1.34 (m, 12H, CH₂), 1.34–1.21 (m, 72H, CH₂), 0.45 and 0.28 (br apparent d, 6H, BH₃); ¹³C{¹H} (126 MHz): 31.0 (d, J_{CP} = 12.0 Hz, CH₂), 29.60 (s, CH₂), 29.58 (s, CH₂), 29.50 (s, CH₂), 29.45 (s, CH₂), 29.2 (s, CH₂), 28.8 (s, CH₂), 22.8 (d, J_{CP} = 34.2 Hz, CH₂), 22.4 (d, J_{CP} = 2.7 Hz, CH₂); ³¹P{¹H} 14.9–13.6 (br s).^{31b} IR (cm^{−1}, powder film): 2915 (s), 2846 (m), 2361 (m), 1468 (m), 1063 (m), 716 (m).

Epimerization of 3b; *in,out*-3b·2BH₃ and (*in,in/out,out*)-3b·2BH₃

A Schlenk flask was charged with (*in,in/out,out*)-3b (0.0488 g, 0.0861 mmol) and mesitylene (10 mL). The solution was stirred at 150 °C. After 60 h, a ³¹P{¹H} NMR spectrum showed a 60 : 40 (*in,in/out,out*)-3b/*in,out*-3b mixture. The solvent was removed by oil pump vacuum, the residue dissolved in THF (15 mL), and Me₂S·BH₃ (2.0 M in THF; 0.30 mL, 0.60 mmol) added with stirring. After 24 h, the solvent was removed by oil pump vacuum. The residue was chromatographed on a silica column (1 × 26 cm) using hexanes/CH₂Cl₂ (1 : 1 v/v). The solvents were removed from the product fractions by oil pump vacuum. First



in,out-3b·2BH₃ eluted (colorless oil, 0.0131 g, 0.0220 mmol, 26%). Anal. calcd for C₃₆H₇₂P₂ (594.57): C, 72.72; H, 13.22; found: C, 73.02; H, 13.13.

NMR (CDCl₃, δ/ppm): ¹H (500 MHz) 1.64–1.54 (m, 12H, CH₂), 1.54–1.45 (m, 12H, CH₂), 1.45–1.37 (m, 12H, CH₂), 1.37–1.24 (m, 36H, CH₂), 0.51 and 0.29 (br apparent d, 6H, BH₃); ¹³C{¹H} (126 MHz) 30.4 (d, J_{CP} = 11.2 Hz, CH₂), 27.7 (s, CH₂), 27.6 (s, CH₂), 27.5 (s, CH₂), 23.4 (d, J_{CP} = 34.3 Hz, CH₂), 22.2 (s, CH₂); ³¹P{¹H} (202 MHz): 15.6–14.1 (br s).^{31b}

Next (*in,in/out,out*)-*3b*·2BH₃ eluted (colorless oil, 0.0194 g, 0.326 mmol, 38%). The NMR data agreed with that from the independent synthesis above.

in,out-P((CH₂)₁₂)₃P (*in,out-3b*)

A Schlenk flask was charged with *in,out-3b*·2BH₃ (0.0070 g, 0.0117 mmol) and pyrrolidine (2 mL). The mixture was refluxed (60 °C) for 3 d. The solvent was removed by oil pump vacuum. Toluene (5 mL) was added, and the suspension passed through a pad of silica gel using a pipette (0.7 × 3 cm). The filter cake was washed with toluene (10 mL). The solvent was removed from the filtrate by oil pump vacuum to give *in,out-3b* (0.0052 g, 0.009 mmol, 77%) as a colorless oil.

NMR (CDCl₃, δ/ppm): ¹H (500 MHz) 1.49–1.36, 1.36–1.23 (2 br m, 72H, CH₂); ¹³C{¹H} (126 MHz) 30.9 (d, J_{CP} = 9.7 Hz, CH₂), 28.7 (s, 2 × CH₂), 28.6 (s, CH₂), 27.0–26.5 (br s, CH₂), 25.5 (d, J_{CP} = 10.6 Hz, CH₂); ³¹P{¹H} (202 MHz) –29.8 to –36.9 (br s) and (from Fig. 2b) –30.1/–40.4 (s/s, 213 K), –29.4/–38.0 (br s/br s, 253 K), –29.2/–36.5 (br s/br s, 273 K), –32.2 (br s, 298 K), –32.3 (br s, 323 K).

Epimerization of *3c*; *in,out-3c*·2BH₃ and (*in,in/out,out*)-*3c*·2BH₃

A Schlenk flask was charged with (*in,in/out,out*)-*3c* (0.252 g, 0.387 mmol) and mesitylene (10 mL). The solution was stirred at 150 °C. After 40 h, a ³¹P{¹H} NMR spectrum showed a 51 : 49 (*in,in/out,out*)-*3c*/*in,out-3c* mixture. The solvent was removed by oil pump vacuum, the residue dissolved in THF (15 mL), and Me₂S·BH₃ (2.0 M in THF; 1.3 mL, 2.6 mmol) added with stirring. After 2 d, the solvent was removed by oil pump vacuum. The residue was chromatographed on a silica column (4 × 46 cm) using hexanes/CH₂Cl₂ (1 : 0 to 0 : 1 v/v). The solvents were removed from the product fractions by oil pump vacuum. First eluted *in,out-3c*·2BH₃ (colorless oil, 0.110 g, 0.162 mmol, 42%). Anal. calcd for C₄₂H₉₀B₂P₂ (678.73): C, 74.32; H, 13.37; found: C, 73.86; H, 13.49.

NMR (CDCl₃, δ/ppm): ¹H (500 MHz) 1.56–1.51 (m, 12H, CH₂), 1.49–1.42 (m, 12H, CH₂), 1.39–1.33 (m, 12H, CH₂), 1.31–1.21 (m, 48H, CH₂), 0.45 and 0.27 (br apparent d, 6H, BH₃); ¹³C{¹H} (126 MHz) 30.5 (d, J_{CP} = 11.3 Hz, CH₂), 28.35 (s, CH₂), 28.28 (s, CH₂), 28.2 (s, CH₂), 28.1 (s, CH₂), 23.0 (d, J_{CP} = 34.3 Hz, CH₂), 22.2 (d, J_{CP} = 1.9 Hz, CH₂); ³¹P{¹H} (202 MHz): 15.8–15.4 (br m).^{31b}

Next eluted (*in,in/out,out*)-*3c*·2BH₃ (colorless oil, 0.114 g, 0.168 mmol, 43%), which solidified to a white powder. The NMR data agreed with that from the independent synthesis above.

in,out-P((CH₂)₁₄)₃P (*in,out-3c*)

A Schlenk flask was charged with *in,out-3c*·2BH₃ (0.048 g, 0.071 mmol) and pyrrolidine (3 mL). The mixture was refluxed (60 °C) for 11 d. The solvent was removed by oil pump vacuum. Toluene (5 mL) was added, and the suspension passed through a pad of silica gel on a Schlenk frit (1.5 × 1 cm). The filter cake was washed with toluene (3 × 4 mL). The solvent was removed from the filtrate by oil pump vacuum to give *in,out-3c* (0.026 g, 0.040 mmol, 56%) as a colorless oil. Anal. calcd for C₄₂H₈₄P₂ (651.06): C, 77.48; H, 13.00; found: C, 77.66; H, 13.09.

NMR (CDCl₃, δ/ppm): ¹H (500 MHz) 1.45–1.35, 1.32–1.23 (2 br m, 84H, CH₂); ¹³C{¹H} (126 MHz) 30.9 (d, J_{CP} = 10.3 Hz, CH₂), 29.0 (s, 2 × CH₂), 28.94 (s, CH₂), 28.86 (s, CH₂), 27.0 (d, J_{CP} = 11.5 Hz, CH₂), 25.6 (d, J_{CP} = 11.8 Hz, CH₂); ³¹P{¹H} (202 MHz) –31.3 (s).

NMR (CDCl₃F, δ/ppm, 263 K): ¹H (500 MHz) 1.46–1.25 (br m, 84H, CH₂); ¹³C{¹H} (126 MHz) 31.0 (d, J_{CP} = 10.3 Hz, CH₂), 29.0 (s, 2 × CH₂), 28.98 (s, CH₂), 28.90 (s, CH₂), 26.8 (d, J_{CP} = 10.9 Hz, CH₂), 25.5 (d, J_{CP} = 11.5 Hz, CH₂); ³¹P{¹H} (202 MHz) –32.5 (s).

³¹P{¹H} NMR (CH₂Cl₂, δ/ppm, 202 MHz selected data from Fig. 2a) –32.3/–37.7 (br s/br s, 183 K), –32.4/–37.4 (br s/br s, 193 K), –34.5 (br s, 208 K), –34.1 (br s, 223 K).

Epimerization of *3e*; *in,out-3e*·2BH₃ and (*in,in/out,out*)-*3e*·2BH₃

A Schlenk flask was charged with (*in,in/out,out*)-*3e* (0.1934 g, 0.2360 mmol) and mesitylene (10 mL). The solution was stirred at 150 °C. After 30 h, a ³¹P{¹H} NMR spectrum showed a 51 : 49 (*in,in/out,out*)-*3e*/*in,out-3e* mixture. The solvent was removed by oil pump vacuum, the residue dissolved in THF (15 mL), and Me₂S·BH₃ (2.0 M in THF; 0.24 mL, 0.48 mmol) added with stirring. After 24 h, the solvent was removed by oil pump vacuum. The residue was chromatographed on a silica column (4 × 46 cm) using hexanes/CH₂Cl₂ (1 : 3 v/v). The solvents were removed from the product fractions by oil pump vacuum. First eluted *in,out-3e*·2BH₃ (colorless oil, 0.0310 g, 0.0366 mmol, 16%). Anal. calcd for C₅₄H₁₁₄B₂P₂ (847.07): C, 76.57; H, 13.57; found: C, 76.53; H, 13.45.

NMR (CDCl₃, δ/ppm): ¹H (500 MHz) 1.59–1.52 (m, 12H, CH₂), 1.52–1.44 (m, 12H, CH₂), 1.41–1.34 (m, 12H, CH₂), 1.34–1.22 (m, 72H, CH₂), 0.49 and 0.29 (br apparent d, 6H, BH₃); ¹³C{¹H} (126 MHz) 31.0 (d, J_{CP} = 11.9 Hz, CH₂), 29.4 (s, CH₂), 29.31 (s, CH₂), 29.28 (s, CH₂), 29.27 (s, CH₂), 29.0 (s, CH₂), 28.8 (s, CH₂), 23.1 (d, J_{CP} = 34.5 Hz, CH₂), 22.5 (d, J_{CP} = 2.4 Hz, CH₂); ³¹P{¹H} (202 MHz): 15.1–13.9 (br s).^{31b}

Next eluted (*in,in/out,out*)-*3e*·2BH₃ (colorless oil, 0.0464 g, 0.0548 mmol, 23%), which solidified (6–8 h) to a white powder. The NMR data agreed with that from the independent synthesis above.

in,out-P((CH₂)₁₈)₃P (*in,out-3e*)

A Schlenk flask was charged with *in,out-3e*·2BH₃ (0.031 g, 0.0366 mmol) and pyrrolidine (2 mL). The mixture was refluxed (60 °C) for 3 d. The solvent was removed by oil pump vacuum.



Toluene (5 mL) was added, and the suspension passed through a pad of silica gel on a Schlenk frit (1.5 × 2 cm). The filter cake was washed with toluene (20 mL). The solvent was removed from the filtrate by oil pump vacuum to give *in,out-3e* (0.0197 g, 0.024 mmol, 66%) as a colorless oil. Anal. calcd for C₅₄H₁₀₈P₂ (819.38): C, 79.15; H, 13.28; found: C, 79.02; H, 13.29.

NMR (CDCl₃, δ/ppm): ¹H (500 MHz) 1.46–1.33, 1.32–1.22 (2 br m, 108H, CH₂); ¹³C{¹H} (126 MHz) 31.2 (d, *J*_{CP} = 10.5 Hz, CH₂), 29.43 (s, CH₂), 29.42 (s, CH₂), 29.39 (s, CH₂), 29.38 (s, CH₂), 29.3 (s, CH₂), 29.1 (s, CH₂), 27.2 (d, *J*_{CP} = 11.9 Hz, CH₂), 25.8 (d, *J*_{CP} = 12.0 Hz, CH₂); ³¹P{¹H} (202 MHz) –31.5 (s).

Conversion of (*in,in/out,out*)-3b to *trans-2b*

A J. Young NMR tube was charged with (*in,in/out,out*)-3b (0.0110 g, 0.0194 mmol), PtCl₂ (0.0054 g, 0.020 mmol), and C₆D₆ (0.6 mL) in a glove box. The mixture was kept at 55 °C for 24 h and chromatographed (SiO₂ column, 0.7 × 3 cm, 5 : 1 v/v hexanes/CH₂Cl₂). The solvent was removed from the product fractions by rotary evaporation to give *trans-2b* (0.0084 g, 0.0101 mmol, 52%) as a yellow powder, mp 160–161 °C. Anal. calcd for C₃₆H₇₂P₂Cl₂Pt (832.89): C, 51.91; H, 8.71; found: C, 53.25; H, 8.98.⁴⁶

NMR (C₆D₆, δ/ppm): ¹H (500 MHz) 1.92–1.82, (br m, 12H, PCH₂CH₂), 1.72–1.62 (br m, 12H, PCH₂CH₂), 1.55–1.41 (br m, 48H, remaining CH₂); ¹³C{¹H} (126 MHz) 30.2 (virtual t, *J*_{CP} = 6.9 Hz, PCH₂CH₂CH₂), 27.9 (s, CH₂), 27.8 (s, CH₂), 27.0 (s, CH₂), 25.4 (virtual t, *J*_{CP} = 16.3 Hz, PCH₂CH₂), 24.3 (s, P CH₂CH₂); ³¹P{¹H} (202 MHz) 9.3 (s, *J*_{PPt} (satellite) = 2442 Hz).

Conversion of (*in,in/out,out*)-3c to *trans-2c*

(A) A round bottom flask was charged with (*in,in/out,out*)-3c (0.0635 g, 0.097 mmol), PtCl₂ (0.0306 g, 0.115 mmol), and CH₂Cl₂ (7 mL) in a glove box. The mixture was stirred for 24 h and chromatographed (SiO₂ column, 1 × 5 cm, 4 : 1 v/v hexanes/CH₂Cl₂). The solvent was removed from the product fractions by rotary evaporation to give *trans-2c* (0.0825 g, 0.090 mmol, 93%) as a yellow powder.⁴⁷ (B) A round bottom flask was charged with *in,in/out,out-3c* (0.0629 g, 0.096 mmol), PtCl₂(NCCH₃)₂ (0.0400 g, 0.115 mmol), and THF (7 mL) in a glove box. The mixture was stirred for 6 h and worked up as in A to give *trans-2c* (0.0835 g, 0.091 mmol, 95%) as a yellow powder.⁴⁷

Conversion of (*in,in/out,out*)-3e to *trans-2e*

A round bottom flask was charged with (*in,in/out,out*)-3e (0.0788 g, 0.096 mmol), PtCl₂ (0.0260 g, 0.098 mmol), and CH₂Cl₂ (10 mL) in a glove box. The mixture was stirred for 24 h and chromatographed (SiO₂ column, 1 × 10 cm, 5 : 1 v/v hexanes/CH₂Cl₂). The solvent was removed from the product fractions by rotary evaporation to give *trans-2e* (0.0719 g, 0.0662 mmol, 69%) as a yellow powder.⁴⁷

Conversion of (*in,in/out,out*)-3c to *trans-PtCl₂(P((CH₂)₁₄)₃P (trans-4c)*

(A) A round bottom flask was charged with *in,in/out,out-3c* (0.0668 g, 0.102 mmol), PdCl₂ (0.0216 g, 0.122 mmol), and

CH₂Cl₂ (7 mL) in a glove box. The mixture was stirred for 24 h and chromatographed (SiO₂ column, 1 × 5 cm, 4 : 1 v/v hexanes/CH₂Cl₂). The solvent was removed from the product fractions by rotary evaporation to give *trans-4c* (0.0795 g, 0.096 mmol, 94%) as a yellow powder.⁴⁵ (B) A round bottom flask was charged with *in,in/out,out-3c* (0.0740 g, 0.113 mmol), PdCl₂(NCCH₃)₂ (0.0311 g, 0.120 mmol), and THF (7 mL) in a glove box. The mixture was stirred for 6 h and worked up as in A to give *trans-4c* (0.0886 g, 0.107 mmol, 95%) as a yellow powder.⁴⁷

Data availability

Additional experimental data are deposited in the ESI† associated with this publication and any further data are available upon request.

Author contributions

All authors except J.A.G. contributed to the experimental work. All authors participated in data analysis. Overall supervision and funding acquisition was carried out by J.A.G. The manuscript was written by J.A.G., Y.Z., and M.S. with contributions by all authors.

Conflicts of interest

The authors declare no competing financial interest.

Acknowledgements

The authors thank the US National Science Foundation (CHE-1153085, CHE-1566601, CHE-1900549) for support, Dr Agnieszka J. Nawara-Hultsch for preliminary observations, Dr Michał Barbasiewicz for assistance with the characterization of (*in,in/out,out*)-3c·2BH₃, and Dr Andreas Ehnborn for helpful discussions and drafting key graphics. This paper is dedicated to Prof. Dr Wolf-Dieter Habicher (Technische Universität Dresden)⁴⁶ on the occasion of his 83rd birthday (31 December 2022).

Notes and references

- 1 L. Fabbizzi, *Cryptands and Cryptates*, World Scientific, Hackensack, New Jersey, 2018. ISBN 9781786343697.
- 2 C. H. Park and H. E. Simmons, Macrobicyclic Amines. II. *out-out* ⇌ *in-in* Prototropy in 1,(*k* + 2)-Diazabicyclo[*k.l.m*] alkaneammonium Ions, *J. Am. Chem. Soc.*, 1968, **90**, 2429–2431. See also the immediately preceding and following communications in this issue.
- 3 R. W. Alder, C. P. Butts, A. G. Orpen, D. Read and J. M. Oliva, Superbasic bridgehead diphosphines: the effects of strain and intrabridgehead P...P bonding on phosphine basicity, *J. Chem. Soc., Perkin Trans. 2*, 2001, 282–287, and references therein.
- 4 R. W. Alder and S. P. East, *In/Out Isomerism*, *Chem. Rev.*, 1996, **96**, 2097–2011.
- 5 S. Kharel, H. Joshi, S. Bierschenk, M. Stollenz, D. Taher, N. Bhuvanesh and J. A. Gladysz, Homeomorphic



- Isomerization as a Design Element in Container Molecules; Binding, Displacement, and Selective Transport of MCl_2 Species ($\text{M} = \text{Pt}, \text{Pd}, \text{Ni}$), *J. Am. Chem. Soc.*, 2017, **139**, 2172–2175.
- 6 Merriam-Webster definition of homeomorphism: a function that is a one-to-one mapping between sets such that both the function and its inverse are continuous and that in topology exists for geometric figures which can be transformed one into the other by an elastic deformation.
 - 7 However, when one assigns an arbitrary 1/2/3 Cahn-Ingold-Prelog priority to each bridge prior to a homeomorphic isomerization, an *R* configured bridgehead remains *R* and an *S* remains *S*, as easily verified with molecular models. Hence, a chiral substrate would not racemize, apropos to a reaction coordinate with no bond breaking or pyramidal inversion.
 - 8 R. D. Baechler and K. Mislow, The Effect of Structure on the Rate of Pyramidal Inversion of Acyclic Phosphines, *J. Am. Chem. Soc.*, 1970, **92**, 3090–3093.
 - 9 (a) R. D. Baechler, J. D. Andose, J. Stackhouse and K. Mislow, Linear Free Energy Correlations of Barriers to Pyramidal Inversion, *J. Am. Chem. Soc.*, 1972, **94**, 8060–8065; (b) J. D. Andose, A. Rauk and K. Mislow, Semiempirical Calculation of Barriers to Pyramidal Inversion. Extension to the Third Row of the Periodic Table, *J. Am. Chem. Soc.*, 1974, **96**, 6904–6907.
 - 10 (a) A. Ehnbon, J. E. Kuszynski, M. B. Hall and J. A. Gladysz, Manuscript in preparation; (b) A. Ehnbon, Doctoral dissertation, Texas A&M University, 2021, Chapter 5.
 - 11 M. Stollenz, D. Taher, N. Bhuvanesh, J. H. Reibenspies, Z. Baranová and J. A. Gladysz, Steric control of the *in/out* sense of bridgehead substituents in macrobicyclic compounds: isolation of new “crossed chain” variants of *in/out* isomers, *Chem. Commun.*, 2015, **51**, 16053–16056.
 - 12 Y. Ikeda, Y. Inagaki and W. Setaka, Simultaneous synthesis and characterization of *in/out*-isomers of disilabicyclo [14.14.14]alkanes, *Chem. Commun.*, 2021, **57**, 7838–7841.
 - 13 See also S. Kharel, T. Jia, N. Bhuvanesh, J. H. Reibenspies, J. Blümel and J. A. Gladysz, A Nontemplated Route to Macrocyclic Dibridgehead Diphosphorus Compounds: Crystallographic Characterization of a “Crossed Chain” Variant of *in/out* Stereoisomers, *Chem. – Asian J.*, 2018, **13**, 2632–2640.
 - 14 (a) A. H. Haines and P. Karntiang, Synthesis of Some *out,in*- and *out,out*-Macrocyclic Polyethers derived from Glycerol. *Out,in-in,out* Isomerism, *J. Chem. Soc., Perkin Trans. 1*, 1979, 2577–2587; (b) R. S. Wareham, J. D. Kilburn, D. L. Turner, N. H. Rees and D. S. Holmes, Homeomorphic Isomerism in a Peptidic Macrobicycle, *Angew. Chem., Int. Ed. Engl.*, 1995, **34**, 2660–2662, Übergangsmetallkomplexe als Wirt und als Gast: Koordination eines Platin-Ammin-Komplexes in zweiter Sphäre an einen Platin-haltigen Azakronenether, *Angew. Chem.*, 1995, **107**, 2902–2904; (c) M. Saunders and N. Krause, The Use of Stochastic Search in Looking for Homeomorphic Isomerism: Synthesis and Properties of Bicyclo[6.5.1]tetradecane, *J. Am. Chem. Soc.*, 1990, **112**, 1791–1795; (d) R. W. Alder, E. Heilbronner, E. Honegger, A. B. McEwan, R. E. Moss, E. Olefirowicz, P. A. Petillo, R. B. Sessions, G. R. Weisman, J. M. White and Z.-Z. Yang, The *out,out* to *out,in* Transition for 1,*(n+2)*-Diazabicyclo [n.3.1]alkanes, *J. Am. Chem. Soc.*, 1993, **115**, 6580–6591.
 - 15 H. Löw, E. Mena-Osteritz, K. M. Mullen, C. M. Jäger and M. von Delius, Self-Assembly, Adaptive Response, and *in,out*-Stereoisomerism of Large Orthoformate Cryptands, *ChemPlusChem*, 2020, **85**, 1008–1012.
 - 16 I. Bauer and W. D. Habicher, *out*-Isomerism of Phosphorus Bridgehead Cage Compounds. A Review, *Collect. Czech. Chem. Commun.*, 2004, **69**, 1195–1230.
 - 17 (a) F. Däbritz, A. Jäger and I. Bauer, Synthesis, Derivatisation and Structural Characterisation of a New Macrobicyclic Phosphane Oxide Cryptand, *Eur. J. Org. Chem.*, 2008, 5571–5576; (b) F. Däbritz, G. Theumer, M. Gruner and I. Bauer, New conformational flexible phosphane and phosphane oxide macrobicycles, *Tetrahedron*, 2009, **65**, 2995–3002.
 - 18 (a) A. J. Nawara-Hultsch, M. Stollenz, M. Barbasiewicz, S. Szafert, T. Lis, F. Hampel, N. Bhuvanesh and J. A. Gladysz, Gyroscope-Like Molecules Consisting of $\text{PdX}_2/\text{PtX}_2$ Rotators within Three-Spoke Dibridgehead Diphosphine Stators: Syntheses, Substitution Reactions, Structures, and Dynamic Properties, *Chem. – Eur. J.*, 2014, **20**, 4617–4637; (b) H. Joshi, S. Kharel, N. Bhuvanesh and J. A. Gladysz, Syntheses, Structures, and Thermal Properties of Gyroscope Like Complexes Consisting of PtCl_2 Rotators Encased in Macrocyclic Dibridgehead Diphosphines $\text{P}((\text{CH}_2)_n)_3\text{P}$ with Extended Methylene Chains ($n = 20/22/30$), and Isomers Thereof, *Organometallics*, 2018, **37**, 2991–3000.
 - 19 (a) H. Joshi, S. Kharel, A. Ehnbon, K. Skopek, G. D. Hess, T. Fiedler, F. Hampel, N. Bhuvanesh and J. A. Gladysz, Three Fold Intramolecular Ring Closing Alkene Metatheses of Square Planar Complexes with *cis* Phosphorus Donor Ligands $\text{P}(\text{X}(\text{CH}_2)_m\text{CH}=\text{CH}_2)_3$ ($\text{X}/m = -/5-10, \text{O}/3-5$); Syntheses, Structures, and Thermal Properties of Macrocyclic Dibridgehead Diphosphorus Complexes, *J. Am. Chem. Soc.*, 2018, **140**, 8463–8478; (b) A workup improvement has raised the yield of *cis*-**2b** in Scheme 3 from 6% to 20–30%, and a revised procedure is supplied in the ESI.†
 - 20 A. Ehnbon, M. B. Hall and J. A. Gladysz, manuscript in preparation.
 - 21 M. Stollenz, M. Barbasiewicz, A. J. Nawara-Hultsch, T. Fiedler, R. M. Laddusaw, N. Bhuvanesh and J. A. Gladysz, Dibridgehead Diphosphines that Turn Themselves Inside Out, *Angew. Chem., Int. Ed.*, 2011, **50**, 6647–6651; M. Stollenz, M. Barbasiewicz, A. J. Nawara-Hultsch, T. Fiedler, R. M. Laddusaw, N. Bhuvanesh and J. A. Gladysz, Dreifach-verbrückte Diphosphine mit von innen nach außen invertierender Konfiguration, *Angew. Chem.* 2011, **123**, 6777–6781.
 - 22 As will be detailed in future papers, solutions stirred under air slowly give diphosphine monoxides and the diphosphine dioxides.
 - 23 G. Petöcz, L. Jánosi, W. Weissensteiner, Z. Csók, Z. Berente and L. Kollár, Synthesis and NMR investigation of



- Pt(CN)₂(diphosphine) and [Pt(CN)(triphosphine)]Cl complexes, *Inorg. Chim. Acta*, 2000, **303**, 300–305.
- 24 Y. Zhu, A. Ehnbohm, T. Fiedler, Y. Shu, N. Bhuvanesh, M. B. Hall and J. A. Gladysz, Platinum(II) Alkyl Complexes of Chelating Dibridgehead Diphosphines P((CH₂)_n)₃P (*n* = 14, 18, 22); Facile *cis/trans* Isomerizations Interconverting Gyroscope and Parachute like Adducts, *Dalton Trans.*, 2021, **50**, 12457–12477.
- 25 Line widths were carefully examined in many series of variable temperature NMR experiments in order to ensure that coalescence phenomena were not being overlooked (e.g., (*in,in/out,out*)-**3c** in CH₂Cl₂ and CDCl₃; (*in,in/out,out*)-**3e** in toluene, CH₂Cl₂, and CDCl₃). Representative data are provided in Fig. S5 and S6.†
- 26 The error limits on the rate constants so derived are commonly viewed as *ca.* 5%, leading to a corresponding uncertainty in the ln(*k*/T) vs. 1/T plots in Fig. S7.† P. M. Morse, M. D. Spencer, S. R. Wilson and G. S. Girolami, A Static Agostic α-CH⋯M Interaction Observable by NMR Spectroscopy: Synthesis of the Chromium(II) Alkyl [Cr₂(CH₂SiMe₃)₆]^{2−} and Its Conversion to the Unusual “Windowpane” Bis(metallacycle) Complex [Cr(κ²C,C′-CH₂SiMe₂CH₂)₂]^{2−}, *Organometallics*, 1994, **13**, 1646–1655.
- 27 While the work was under review, a new synthetic route to **3** was developed that furthermore allows access to the smaller macrocycle P((CH₂)₁₀)₃P (**3a**).²⁸ This species again shows two ³¹P{¹H} NMR signals (*ca.* −32 and −39 ppm, mesitylene), but now the upfield peak (assigned to the *out,out* isomers of **3b**, **3c**) dominates. This is in accord with the expected crossover to more stable *out,out* isomers as the ring size decreases, strengthening all proposed assignments.
- 28 S. R. Zarcone and J. A. Gladysz, manuscript in preparation.
- 29 M. Saunders, Stochastic Search for the Conformations of Bicyclic Hydrocarbons, *J. Comput. Chem.*, 1989, **10**, 203–208.
- 30 A second mechanistic test is in theory possible. When one assigns an arbitrary 1/2/3 Cahn-Ingold-Prelog priority to each bridge prior to a double pyramidal inversion, an *R* configured bridgehead inverts to *S* and an *S* becomes *R* (racemization). As noted above, a homeomorphic isomerization of such an educt would proceed with retention.⁷
- 31 (a) J. M. Brunel, B. Faure and M. Maffei, Phosphane-boranes: synthesis, characterization, and synthetic applications, *Coord. Chem. Rev.*, 1998, **178–180**, 665–698, see section 5.1.2.; (b) While the overall shapes of the P⋅BH₃ ³¹P{¹H} and ¹H NMR signals of **3b**, **c**, **e**-2BH₃ (e.g., Fig. S10 and S11†) are in accord with those in the literature, most couplings are not resolved.
- 32 Independent but much longer and lower yielding syntheses of these compounds are briefly described in the discussion section: see T. Fiedler, M. Barbasiewicz, M. Stollenz and J. A. Gladysz, Non-Metal-Templated Approaches to bis(Borane) Derivatives of Macrocyclic Dibridgehead Diphosphines via Alkene Metathesis, *Beilstein J. Org. Chem.*, 2018, **14**, 2354–2365.
- 33 The methylcyclopentane was unexpected as the crystals were grown from a hexanes solution. However, methylcyclopentane is often a significant component of technical grade hexanes. Of the several methylcyclopentane solvates in the Cambridge Structural Database, at least one was also obtained from hexanes: M. Vale, M. Pink and A. Rajci, Synthesis, Structure, and Conformation of Aza[1_n]metacyclophanes, *J. Org. Chem.*, 2008, **73**, 27–35, see pages S4, S12 therein.
- 34 M. Stollenz, N. Bhuvanesh, J. H. Reibenspies and J. A. Gladysz, Syntheses and Structures of Digold Complexes of Macrobicyclic Dibridgehead Diphosphines that can turn themselves Inside Out, *Organometallics*, 2011, **30**, 6510–6513.
- 35 (a) A. E. Estrada, Y. Wang, N. Bhuvanesh, F. Hampel and J. A. Gladysz, Syntheses, Structures, Reactivities, and Dynamic Properties of Gyroscope Like Complexes Consisting of Rh(CO)(X) or Rh(CO)₂(I) Rotators and Cage Like *trans* Aliphatic Dibridgehead Diphosphine Stators, *Organometallics*, 2022, **41**, 733–749; (b) A. L. Estrada, Y. Wang, G. Hess, F. Hampel and J. A. Gladysz, Square Planar and Octahedral Gyroscope-Like Metal Complexes Consisting of Dipolar Rotators Encased in Dibridgehead Di(triaryl)phosphine Stators: Syntheses, Structures, Dynamic Properties, and Reactivity, *Inorg. Chem.*, 2022, **61**, DOI: [10.1021/acs.inorgchem.2c02855](https://doi.org/10.1021/acs.inorgchem.2c02855).
- 36 S. R. Zarcone, P. J. Verardi, N. Bhuvanesh and J. A. Gladysz, A Surprise Landing on the *Terra Incognita* of Macrocyclic Dibridgehead Diorganoarsines: Syntheses, Structures, and Reactivities, *Chem. Commun.*, 2022, **58**, 8694–8697.
- 37 (a) T. L. Walker, I. S. Taschner, S. M. Chandra, M. J. Taschner, J. T. Engle, B. R. Schrage, C. J. Ziegler, X. Gao and S. E. Wheeler, Lone-Pair-Induced Topicity Observed in Macrobicyclic Tetra-thia Lactams and Cryptands: Synthesis, Spectral Identification, and Computational Assessment, *J. Org. Chem.*, 2018, **83**, 10025–10036; (b) I. S. Taschner, T. L. Walker, S. M. Chandra, B. R. Schrage, C. J. Ziegler, X. Gao and S. E. Wheeler, Topomeric aza/thia cryptands: synthesis and theoretical aspects of *in/out* isomerism using *n*-alkyl bridging, *Org. Chem. Front.*, 2020, **7**, 1164–1176.
- 38 M. L. Connolly, Solvent-accessible surfaces of proteins and nucleic-acids, *Science*, 1983, **221**, 709–713.
- 39 L. Liu and Q.-X. Guo, Isokinetic Relationship, Isoequilibrium Relationship, and Enthalpy-Entropy Compensation, *Chem. Rev.*, 2001, **101**, 673–696.
- 40 (a) R. W. Alder and D. Read, Remarkable *In/out* Inversions at Bridgehead Phosphorus Atoms, *Angew. Chem., Int. Ed.*, 2000, **39**, 2879–2882; *Angew. Chem.*, 2000, **112**, 3001–3004; (b) See also R. W. Alder, C. P. Butts, A. G. Orpen and D. Read, Bridgehead phosphorus chemistry: *in-out* inversion, intrabridgehead P⋯P bonding, and reactivity, *J. Chem. Soc., Perkin Trans. 2*, 2001, 288–295.
- 41 S. R. Zarcone, N. Bhuvanesh and J. A. Gladysz, Unpublished crystal structures.



- 42 A. Ehnborn and J. A. Gladysz, Gyroscopes and the Chemical Literature, 2002-2020: Approaches to a Nascent Family of Molecular Devices, *Chem. Rev.*, 2021, **121**, 3701–3750.
- 43 C. Brown, B. T. Heaton and J. Sabounchei, Oxidative addition reactions of $[\text{Pt}(\text{CN})_4]^{2-}$; A ^{13}C and ^{195}Pt NMR study, *J. Organomet. Chem.*, 1977, **142**, 413–421.
- 44 C. Mühle, J. Nuss and M. Z. Jansen, Crystal Structure of Tetracyanoplatinate(IV) dihydrate, $\text{Pt}(\text{CN})_4 \cdot 2\text{H}_2\text{O}$, *Z. Kristallogr. – New Cryst. Struct.*, 2009, **224**, 9–10.
- 45 J. S. Siegel and F. A. L. Anet, Dichlorofluoromethane- d_2 : a versatile solvent for VT-NMR experiments, *J. Org. Chem.*, 1988, **53**, 2629.
- 46 Although this sample did not give a satisfactory microanalysis, the best available data are given. It was judged to be >96% pure by NMR.
- 47 The ^1H and $^{31}\text{P}\{^1\text{H}\}$ NMR spectra (CDCl_3) were identical with those reported earlier.^{18a}

